TECHNICAL NOTES

NATIONAL ADVISORY COMMITTEE FOR AERONAUTICS

No. 908

SOME INVESTIGATIONS OF THE GENERAL INSTABILITY OF STIFFENED METAL CYLINDERS

IV - CONTINUATION OF TESTS OF SHEET-COVERED SPECIMENS AND STUDIES OF THE BUCKLING PHENOMENA OF UNSTIFFENED CIRCULAR CYLINDERS

Guggenheim Aeronautical Laboratory
California Institute of Technology

Washington
August 1943

NATIONAL ADVISORY COMMITTEE FOR AERONAUTICS

TECHNICAL NOTE NO. 908

SOME INVESTIGATIONS OF THE GENERAL INSTABILITY OF STIFFENED METAL CYLINDERS

IV - CONTINUATION OF TESTS OF SHEET-COVERED SPECIMENS AND STUDIES OF THE BUCKLING PHENOMENA OF UNSTIFFENED CIRCULAR CYLINDERS

Guggenheim Aeronautical Laboratory
California Institute of Technology

This is the fourth of a series of reports covering an investigation of the general instability problem by the California Institute of Technology. The first five reports of this series cover investigations of the general instability problem under the loading conditions of pure bending and were prepared under the sponsorship of the Civil Aeronautics Administration. The succeeding reports of this series cover the work done on other loading conditions under the sponsorship of the National Advisory Committee for Aeronautics.

INTRODUCTION

This report is to deal primarily with the continuation of tests of sheet-covered specimens and studies of the buckling phenomena of unstiffened circular cylinders. The earlier work on this investigation of the problem of general instability of stiffened metal cylinders at C.I.T. has been reported in references 1, 2, and 3. Tests have been completed on the first series of sheet-covered specimens. The longitudinals and frames of the sheet-covered specimens were identical to those of the wire-braced specimens discussed in reference 3. The sheet covering was in all cases 0.010-inch 17S-T dural. The longitudinal spacing was varied from 2.53 to 10.12 inches and the frame spacing from 1 to 16 inches. An attempt has been

made to correlate the experimental data of the wire-braced and sheet-covered specimens. A detailed discussion is given in the discussion of the normal restraint coefficient in this report. Ryder's theoretical work has been applied to three specimens. The results are tabulated in table III and discussed in the body of the report.

In addition to the results on the sheet-covered specimens, the results of an investigation on axially loaded thin-wall metal cylinders will be included in this report. As the preliminary work of this investigation was discussed in reference 2, only results of the more recent work are included. An important finding of this investigation has been the determination of the initial wave form. It has been found that the initial wave form does not agree with the uniform sinusoidal type of wave which has been previously assumed for the theoretical solution, but is elliptical in shape, scattered at random through the cylinder, and changes to a diamond shape as the load is increased.

EXPERIMENTAL INVESTIGATION OF SHEET-COVERED SPECIMENS

As pointed out in reference 2, a number of sheet-covered specimens were to be tested to determine whether or not a correlation could be obtained between the failing bending moments of the wire-braced and the sheet-covered specimens. The construction of the sheet-covered and wire-braced specimens was essentially similar, the only difference being that the wire bracing was replaced by the sheet. Details of construction and test procedure have been discussed in detail in reference 2 and will not be repeated here.

Table I gives the complete set of sheet-covered specimens which have been tested, the number of frames and longitudinals in each specimen, the failing bending moment, the critical compressive longitudinal stress, and the restraint coefficient. Specimens 25 to 28 were discussed in reference 3, and specimens 29 to 39 have been tested since that report was written.

Specimen 29 failed by panel instability; the tabulated compressive stress is that at which buckling between frames started and corresponds to a moment of 66,000 inch-pounds. Because of the symmetrical buckling of the longitudinals, transverse stresses were set up in the sheet.

As the amplitudes of the longitudinals increased, the transverse stresses became larger and the stabilizing effect of the sheet increased. This stabilizing effect of the sheet on the longitudinals was quite evident at the higher loads, as illustrated in figures 2 and 38, and prevented collapsing of the specimen. The bending moment was increased to 123,000 inch-pounds without any definite failure. Specimens 28 and 34 started to fail by panel instability; however, upon increasing the bending moment the frames failed at the tabulated bending moment. The loads at which panel instability occurred were 140,000 and 45,000 inch-pounds, respectively.

In figure 4 the compressive failing stress, which is discussed later, is plotted as a function of the longitudinal spacing b, for constant values of d/b, referred to as "aspect ratio." It is of considerable interest to note that each curve is displaced by a contraction or expansion of the abscissa. The regularity of this family of curves would indicate that such a parameter exists that if the compressive stress is plotted as a function of this parameter a single curve would be obtained. If such a parameter can be found, a limiting value could be established which would indicate the transition region between panel instability and general instability. A number of parameters have been attempted, but as yet the results have not been very successful. In figure 37 the failing compressive stress has been plotted as a function of $\sqrt[3]{\frac{I_{\sigma_f}}{d}\frac{I_{\sigma_l}}{b}}$ the parameter suggested by Dschou's work. (See reference 1, p. 12). The resulting curve indicates a linear relationship.

In calculating I_{σ_l} and I_{σ_f}, the following assumptions were made:

1. The effective width of sheet acting with each longitudinal can be calculated by Marguerre's equation,

$$\frac{w_e}{b} = \frac{1}{2}\sqrt{\frac{\sigma_l}{\sigma}}$$

where

σ_l longitudinal stress

σ_b buckling stress of sheet

2. The effective width of sheet acting with the frame is equal to the effective width of sheet acting with the longitudinal.

I_{σ_l} is then the moment of inertia of the longitudinal plus an effective width of sheet corresponding to the longitudinal stress σ, and I_{σ_f} is the moment of inertia of the frame plus an effective width of sheet equal to that acting with the longitudinal. In view of these rather arbitrary assumptions, too much confidence should not be placed in this curve until further investigations have been carried out on the effects of changing the sheet thickness, and the stiffness of the frames and the longitudinals.

Ryder's analysis could be applied only to three specimens: namely, 25, 26, and 27, as the parameters of the other specimens lie outside the range covered by the published charts. The results for these three specimens are given in table III. In all three cases the calculated panel instability stress is larger than the calculated general instability stress; hence the method predicted correctly the occurrence of general instability. The predicted instability stress and the experimental value are in good agreement for specimen 27; for specimens 25 and 26 the predicted stresses are considerably lower than the experimental stresses.

An extensive comparison between the theoretically predicted general instability stresses and the experimentally obtained stresses will be given after tests have been conducted on specimens in which the sheet thickness and the stiffness of the frames and the longitudinals have been varied.

MAXIMUM STRESSES IN THE LONGITUDINALS

In the first sheet-covered specimens an attempt was made to measure the stresses in the longitudinals with Huggenberger extensometers. The stress measurements as indicated by the curves in figures 13 to 16 have not been very successful. Various methods of attaching the instruments to the longitudinals have been tried; however, the irregularity of the stress measurements has not been eliminated. A method of measuring the maximum stresses which has been adopted is to measure the over-all maximum

deflections of the specimen by means of dial gages, as shown in the photographs (figs. 3 and 38 to 47). If the elastic modulus of the longitudinals and the over-all strain are known, the stresses can be calculated. Since the radial deflections of the stiffeners are measured for various increments of load, the maximum stress can be correctly calculated, even for cases in which radial deflection occurs, by means of the equation

$$\sigma = \frac{\Delta L E}{L} - \frac{E}{2L} \int_0^L \left(\frac{\partial w}{\partial x}\right)^2 dx$$

where

σ stress, pounds per square inch

ΔL total over-all deflection, inches

L length of the specimen, inches

w radial deflection, inches

The expression $\frac{E}{2L} \int_0^L \left(\frac{\partial w}{\partial x}\right)^2 dx$ is the correction for the deflection caused by the wave form of the longitudinals. It has been found that, in general, the correction due to the curvature (M/EI) is quite small; however, for cases in which the longitudinals buckle between frames, the correction becomes quite appreciable. These corrections were made in the measured over-all deflections of specimen 34. The results of this latter type of stress measurement are shown in figures 8 to 12, in which the stress is plotted as a function of the applied bending moment. It is felt that these results are more reliable than those obtained from the extensometer readings. One disadvantage is that only the maximum stresses are measured; however, in the majority of cases only the maximum stresses are of primary importance.

The compressive stress curve in figure 12 is rather interesting in that three definite breaks occur in the curve. It seems logical to assume that the first break is due to buckling of the sheet between longitudinals,

the second to buckling of the sheet between rivets, and the third to the stress exceeding the proportional limit of the material.

A new method of calculating the actual stress which occurs in the longitudinals of stiffened cylinders subjected to pure bending has been recently developed by H. L. Cox (reference 4). Stress calculations based on this method are in excellent agreement with the above-described measured stresses. The tabulated stresses for specimens 25, 26, and 28 were not measuredbut merely calculated by this method; the stress for specimen 28 was calculated on the basis of 168,000 inch-pounds bending moment, assuming no buckling of the longitudinals.

THE NORMAL RESTRAINT COEFFICIENT P/δ

The resistance of a stiffened cylinder to an externally applied radial load has been discussed in detail in reference 3. As stated in the concluding remarks, further experimental evidence was necessary to establish the validity of P/δ as a correlation parameter for the wire-braced and sheet-covered specimens. It was also thought that this parameter might aid in predicting the failing load of a specimen without applying any load to the structure other than the loads necessary to obtain the P/δ values. A plot of failing bending moment as a function of P/δ for all the sheet-covered specimens and for a number of the wire-braced specimens is shown in figure 5. This plot indicates that the expected general relationship does not hold, inasmuch as the failing bending moment is not only a function of P/δ but also varies with the longitudinal spacing. The linear relationship, however, holds between certain limits. For the sheet-covered specimens, the relation is linear with the exception of the 1-inch frame spacing, which is an extreme case and can hardly be expected to conform. For the wire-braced specimens the relationship is, in general, nonlinear. It should be noted that for the 5.06- and 10.12-inch longitudinal spacing the values of P/δ differ by only a few percent. To investigate further the effect of longitudinal spacing, the P/δ value was obtained for a specimen in which the longitudinal spacing was 50.6 inches - that is, only the top and the bottom longitudinals remained. The curves of P against δ for this specimen and for a specimen having a 10.12-inch longitudinal spacing

are shown in figure 7. The difference in the initial slopes — that is, P/δ, is only 5 percent. The small difference which exists in the P/δ value as the spacing of the longitudinals is varied from 5.06 to 50.6 inches leads to the conclusion that after a certain longitudinal spacing, lying between 2.53 and 5.06 inches, P/δ is no longer a measure of the resistance of the specimen as a whole to an externally applied load but rather the resistance of a single longitudinal. The critical longitudinal compressive stress has also been plotted as a function of P/δ in figure 6. Only the sheet-covered specimens having a 2.53- and a 5.06-inch longitudinal spacing scatter around a common curve.

There are, therefore, two difficulties in using P/δ as a correlation parameter for the failing moment:

1. It is evident that the elastic characteristics of the stiffened cylinder are determined by the longitudinal and the circumferential stiffnesses. The measurement of P/δ gives only something like the mean stiffness in these two directions. If the failing moment is a function of the same mean stiffness, then the failing moment will be a function of P/δ only. If this is not true, then some other parameter like d/b (aspect ratio of stiffening) must be used with P/δ. This is confirmed by the experiments, as shown in figure 5.

2. It is also evident from figure 5 that the value of P/δ changes very slowly when the longitudinal spacing is large, while the failing moment changes very rapidly. Thus the failing moment against P/δ curve, at a constant d/b ratio, is very steep when the longitudinal spacing is large. Therefore, a small error in the P/δ determination gives a large error in the failing moment. It should, however, be kept in mind that the 10-inch longitudinal spacing is already considerably larger than that which would be encountered in practice for geometrically equal structures.

At present, there is no evidence of a reasonable correlation parameter between the sheet-covered and the wire-braced specimens, and it probably will be necessary to continue the experimental work with sheet-covered specimens.

DEFLECTION OF THE LONGITUDINALS

The deflection curves of the longitudinals, after failure of the specimen, are shown in figures 17 to 34. A marked difference has been observed in the type of failure of the wire-braced and sheet-covered specimens. Failure of the wire-braced specimens was in general a gradual process - that is, the specimens tend to approach a maximum bending moment in an asymptotic manner. The failure, however, of the sheet-covered specimens is characterized by a sudden and violent collapsing of the specimen. The radial deflection of the longitudinals, for longitudinal spacings less than 16 inches, is practically zero up to the failing load. A number of photographs (figs. 38 to 47) also are included to illustrate further the failure pattern of the longitudinals and the frames.

EXPERIMENTAL INVESTIGATIONS ON COMPRESSIVE FAILING STRESS OF UNSTIFFENED CIRCULAR CYLINDERS

In the discussion of the strength of axially loaded, unstiffened cylinders (reference 1) it was pointed out that a very poor agreement exists between experimental results and those calculated by the classical buckling theories for circular cylinders. This was especially true for large values of R/t. It was also found that very little information was available on the effect of length, particularly for values of $L/R < 1$.

In view of the need for additional information concerning these two parameters a systematic investigation was carried out on steel cylinders in which the R/t ratios were higher than had been previously investigated and on cylinders whose lengths were less than the radius. The specific parameters involved in this investigation were:

1. the radius-thickness ratio R/t
2. the length-radius ratio L/R
3. the critical stress-elastic modulus ratio σ/E

The specimens tested were all fabricated from standard shim stock steel in which the norminal thickness was varied from 0.002 to 0.009 inch. Since the fabricated cylinders had a radius of 6.375 inches the R/t range varied from 750 to 3000. The L/R ratio was varied from 0.1 to 1.5.

The ends of the test cylinder were rigidly clamped into steel end plates, giving fixed end support to the axial fibers of the cylinder. The test apparatus is shown in figures 48 and 49. The load was applied by means of the screw jack and transmitted through the ring, which measures the load, to the cylinder. To prevent any horizontal components of load, the ring was mounted on a spherical ball joint.

The test results are shown in figures 35 and 36, in which σ/E is plotted as a function of L/R for constant values of R/t.

where

σ failing stress, pounds per square inch

E Young's modulus, pounds per square inch

An empirical equation was developed to fit the experimental points. The equation is essentially of the same form as the Wagner empirical design formula (reference 5), inasmuch as the variables used are t/R and t/L; however, the coefficients and exponents have been modified to read:

$$\frac{\sigma}{E} = 9(t/R)^{1.6} + 0.16(t/L)^{1.3}$$

A plot of this equation for values of R/t and L/R corresponding to the range of the experimental investigation is shown by the curves in figures 35 and 36. For values of L/R greater than 1.5 experimental results indicate that σ/E is for all practical purposes a constant.

These experimental results are again at variance with the theoretical investigation of W. Flügge as cited by S. Timoshenko. (See reference 1.) The classical theory of W. Flügge shows that the length effect is negligible

until L/mR is lower than 0.2, where m is the number of half-waves in the axial direction. Since the edges of the test specimens were clamped, it is evident that $m = 2$ for the short cylinders. According to the classical theory, therefore, the length effect is negligible until L/R is less than 0.4. This is another failure of the classical theory of thin shells to predict correctly the behavior of buckling phenomena.

Since the physical properties of the shim stock varied for every thickness, it was necessary to determine experimentally the modulus of elasticity for each thickness. The results are tabulated in table II. The stress-strain relation was obtained for the material in tension; the tension load was applied, with reference to the grain structure of the material, in the same direction as the compression load in the test cylinder.

DETAILED STUDY OF BUCKLING PHENOMENA OF CYLINDRICAL SHELLS

The relatively large discrepancies between the theoretically predicted and the experimentally obtained buckling loads have led to the conclusion that some of the assumptions made in the theoretical treatment of the problem may be at variance with the actual conditions. Hence, to obtain a better understanding of the mechanism involved in the failure of thin-wall cylinders, it was felt that it would be desirable to determine the exact shape of the initial waves which appear in the test cylinder. This was accomplished by restraining the loading mechanism so that any desired over-all deflection could be maintained at any stage of the loading.

The test apparatus is shown in figures 50 to 52. The three upper set screws afford adjustment of the loading head and rest on a 3/4-inch plate. This plate, in turn, is held in position by three 1/2-inch screws resting on the base plate and turned by means of the gear system shown. This lowers or raises the 3/4-inch plate as desired. The small 2-inch central gear, which turns the three 5-inch diameter gears, can be externally operated. In this manner the motion of the loading head can be arrested at any desired position during loading of the specimen.

The progressive change in the wave shape and the wave pattern is indicated in figures 53 to 64. The first specimen, designated as C-1 to C-6 in the figures, was 9 inches long with a 0.0034-inch wall thickness. The second specimen, C-8 to C-13, was 6 inches long with a 0.0034-inch wall thickness.

It should be noted that the wave pattern does not agree with the uniformly distributed sinusoidal type of wave which has been previously assumed for the theoretical solution. The initial wave form is elliptical in shape and scattered at random through the specimen. As the load is increased, the waves tend toward a diamond shape and move to a more uniform configuration. The discrepancy between the actual and the assumed wave form may account for the large difference in the theoretically predicted and the experimentally obtained buckling load.

Guggenheim Aeronautical Laboratory,
California Institute of Technology,
Pasadena, Calif., September 1939.

REFERENCES

1. Guggenheim Aeronautical Laboratory, California Institute of Technology: Some Investigations of the General Instability of Stiffened Metal Cylinders I – Review of Theory and Bibliography. T.N. No. 905, NACA, 1943.

2. Guggenheim Aeronautical Laboratory, California Institute of Technology: Some Investigations of the General Instability of Stiffened Metal Cylinders II – Preliminary Tests of Wire-Braced Specimens and Theoretical Studies. T.N. No. 906, NACA, 1943.

3. Guggenheim Aeronautical Laboratory, California Institute of Technology: Some Investigations of the General Instability of Stiffened Metal Cylinders. III - Continuation of Tests of Wire-Braced Specimens and Preliminary Tests of Sheet-Covered Specimens. T.N. No. 907, NACA, 1943.

4. Cox, H. L.: Stress Analysis of Thin Metal Construction. R.A.S., vol. XLIV, March 1940.

5. Ballerstedt, W., and Wagner, H.: Versuch über die Festigkeit dünner Unversteifter Zylinder. Luftfahrtforschung, 1936, p. 309.

TABLE I

PURE BENDING TESTS OF LONGITUDINALS - FRAME COMBINATIONS

[All longitudinals S_1; all frames F_5]

Test	Longitudinal spacing, b (in.)	Frame spacing, d (in.)	Number of frames in 64 in.	P/δ	Failing moment M.B. (in.-lb)	Max. compressive stress at failure	Type of failure
25	2.53	8	7	330	219,000	16,200	General instability.
26	2.53	4	15	450	274,000	19,400	Do.
27	2.53	2	31	614	359,000	25,600	Do.
28	2.53	16	3	255	168,500*	13,000	Started by panel instability - final failure general instability.
29	5.06	16	3	222	123,000*	6,600**	Panel instability.
30	5.06	8	7	257	107,500	12,200	General instability.
31	5.06	4	15	350	137,500	16,500	Do.
32	5.06	2	31	510	185,000	22,200	Do.
34	10.12	16	3	209	50,000	8,200	Started by panel instability - final failure general instability.
35	10.12	8	7	261	60,000	10,500	General instability.
36	10.12	4	15	361	75,000	14,200	Do.
37	10.12	2	31	476	100,000	17,800	Do.
38	5.06	1	63	740	209,000	26,000	Do.
39	2.53	1	63	815	397,000	29,600	Do.

*Failing bending moment.
**Panel instability stress.

TABLE II

VARIATIONS OF YOUNG'S MODULUS

WITH THICKNESS

Nominal thickness (in.)	Young's modulus (lb/sq in.)
0.002	33.5×10^6
.003	32.0
.004	32.4
.005	31.5
.006	30.6
.0085	29.0

TABLE III

CALCULATION OF CRITICAL STRESS BY RYDER'S METHOD

FOR SHEET-COVERED SPECIMENS

Specimen	Longitudinal spacing, b (in.)	Frame spacing d (in.)	Max. compressive stress at failure, $(\sigma_{cr})_{exp}$	$\frac{\sigma_{cr}}{\sigma_b}$	$\frac{I_{\sigma f}/I_{of}}{I_{\sigma l}/I_{ol}}$	K_1	$K_2=\frac{I_{\sigma f}b}{K_1 I_{\sigma l} d}$	$\frac{A_{\sigma f}}{A_{\sigma l}}$	$K_3=\frac{A_{\sigma f}b}{K_1 A_{\sigma l} d}$	$K_4=\frac{G't b}{E K_1 A_l}$	t_o/ρ_l (from Ryder's curves)	Calculated critical stress (lb/sq in.)
27	2.53	2	25,600	6.40	1.29	1.30	0.0541	0.915	0.894	0.101	0.50	22,290
26	2.53	4	19,400	5.88	1.29	1.30	.0270	.922	.448	.100	.30	13,380
25	2.53	8	16,200	5.40	1.30	1.30	.0135	.917	.223	.100	.18	8,410

NOTE:

All figures are four times actual size

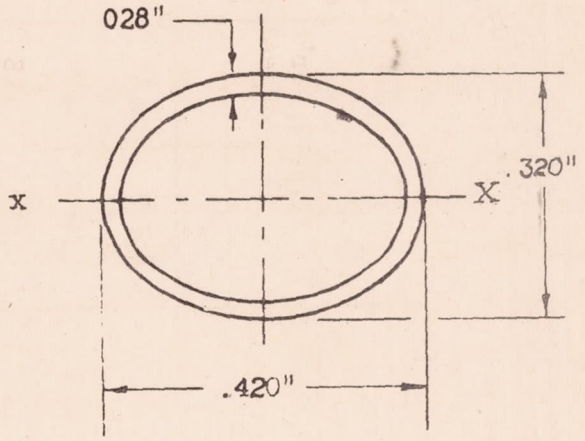

STIFFENER - S_1

AREA = .0324 sq.in. I_{xx}=.000374 in.^{4}

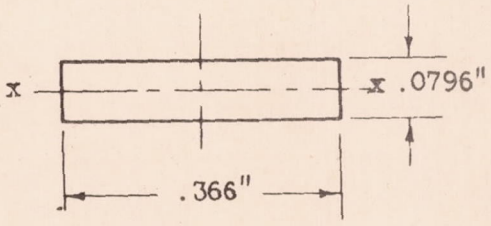

FRAME - F_5

AREA =.0291 sq.in. $I_{xx} = 1.557 \times 10^{-5}$

FIGURE 1

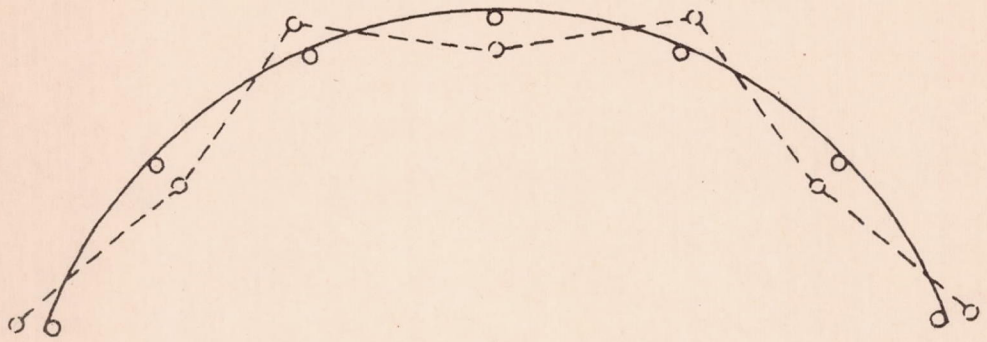

FIGURE 2

Deflection pattern of longitudinals causing transverse stresses to be set up in the sheet.

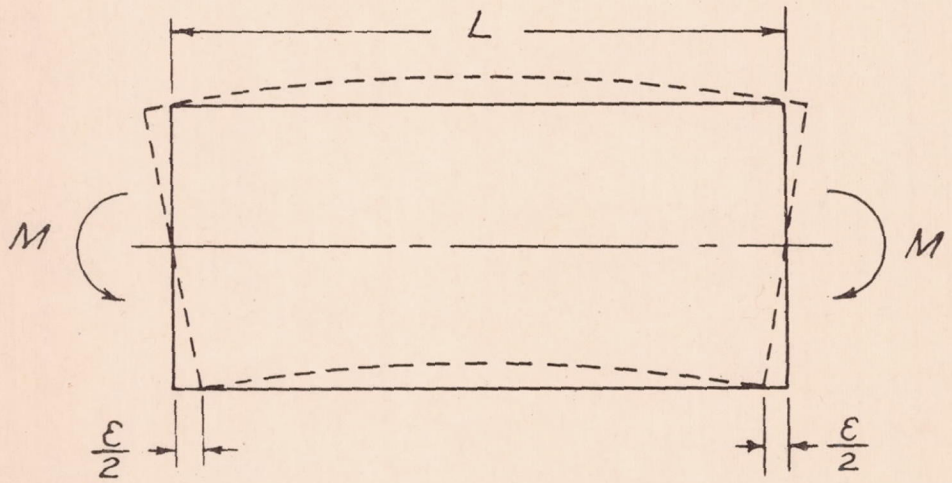

FIGURE 3

Diagram showing measurement of overall axial deflection.

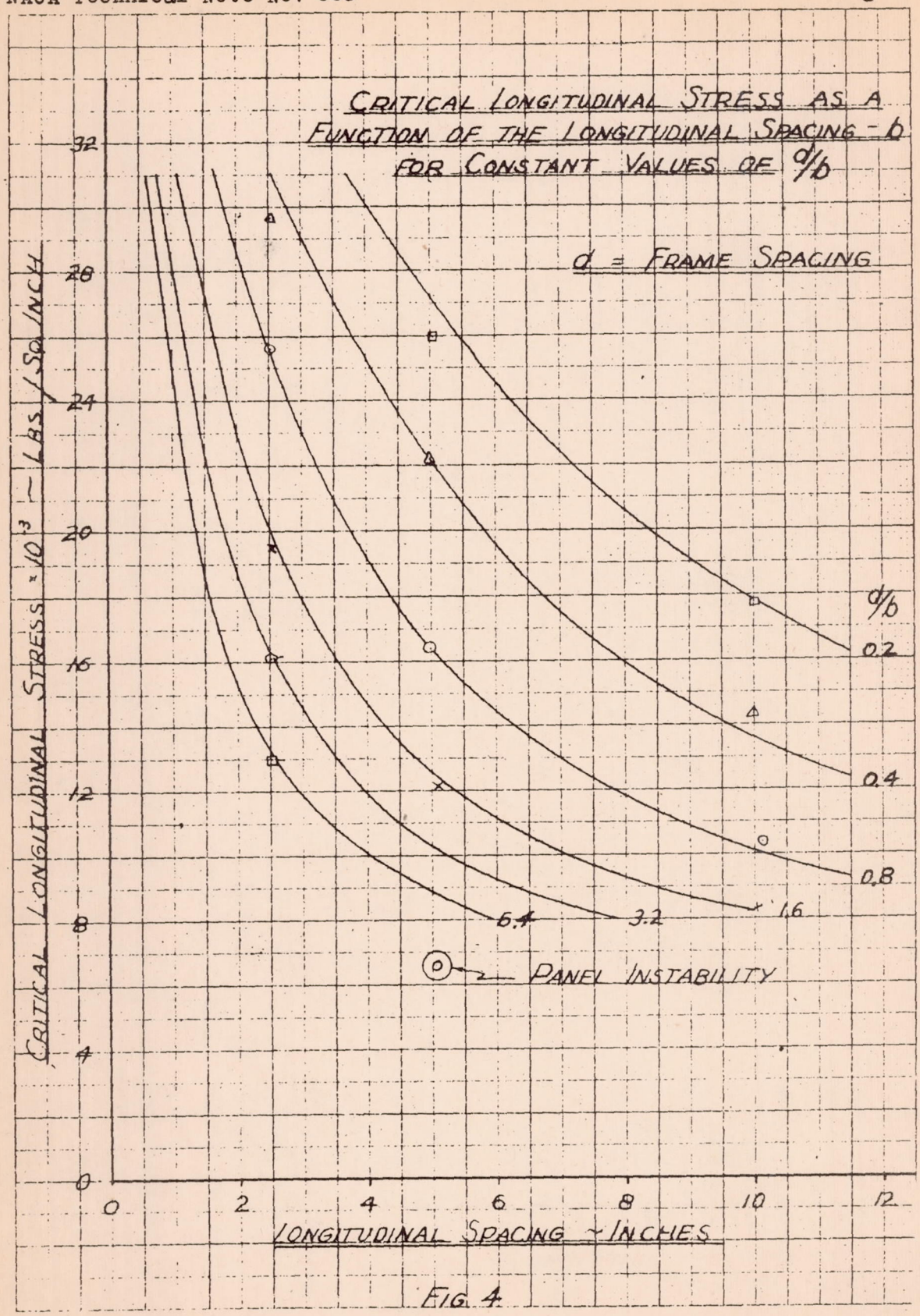
CRITICAL LONGITUDINAL STRESS AS A FUNCTION OF THE LONGITUDINAL SPACING - b FOR CONSTANT VALUES OF d/b
d = FRAME SPACING
CRITICAL LONGITUDINAL STRESS - 10^3 - LBS./SQ.INCH
LONGITUDINAL SPACING - INCHES
d/b
0.2
0.4
0.8
1.6
3.2
6.4
PANEL INSTABILITY
0
4
8
12
16
20
24
28
32
0
2
4
6
8
10
12

FIG. 4

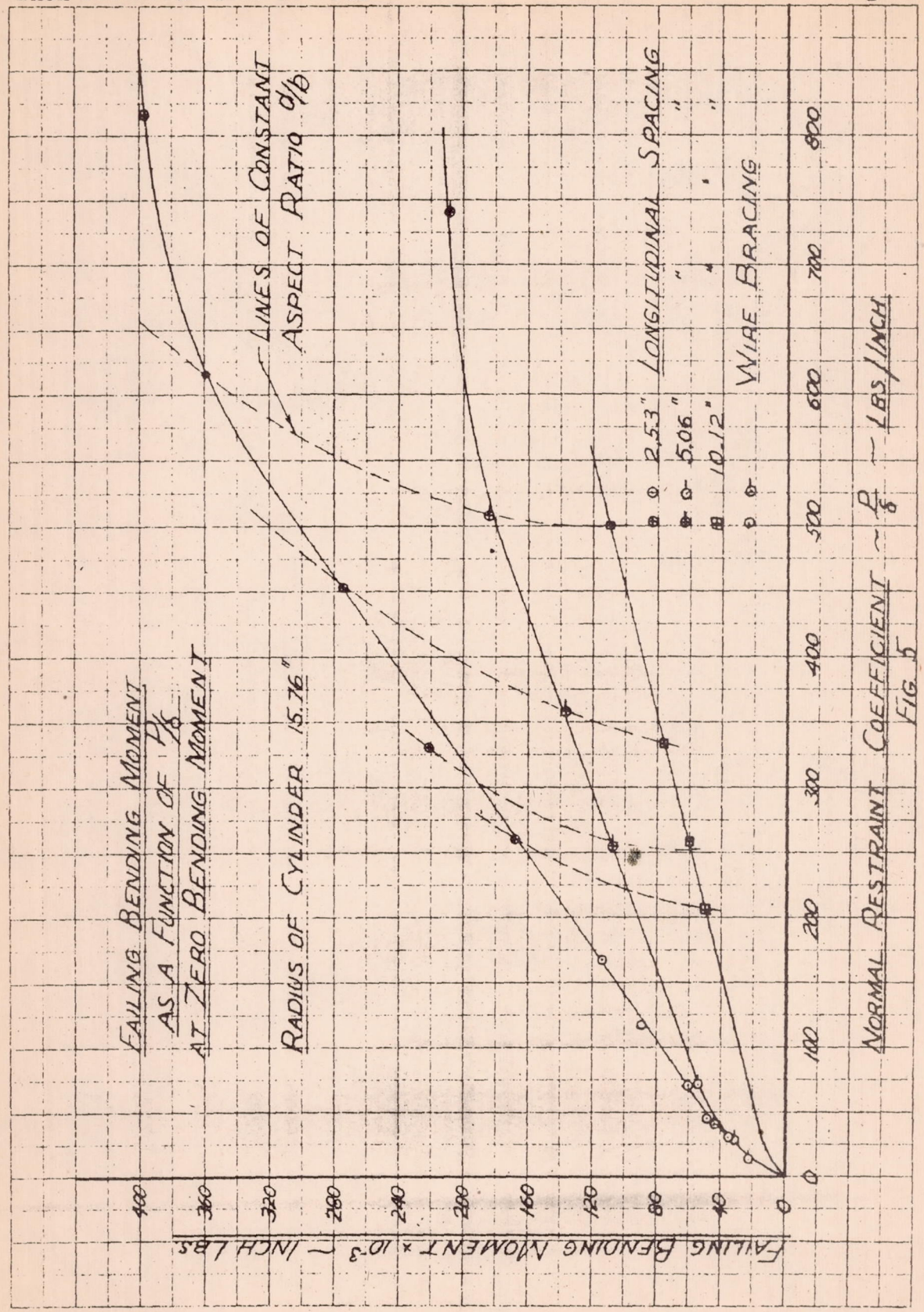
Failing Bending Moment P/δ
As a Function of P/δ
At Zero Bending Moment
Radius of Cylinder 15.76"
Lines of Constant Aspect Ratio d/b
Failing Bending Moment × 10^3 ~ Inch Lbs.
Normal Restraint Coefficient ~ P/δ ~ Lbs./Inch
Fig. 5
Wiae Bracing
2.53" Longitudinal Spacing
5.06" " "
10.12" " "
0
40
80
120
160
200
240
280
320
360
400
0
100
200
300
400
500
600
700
800

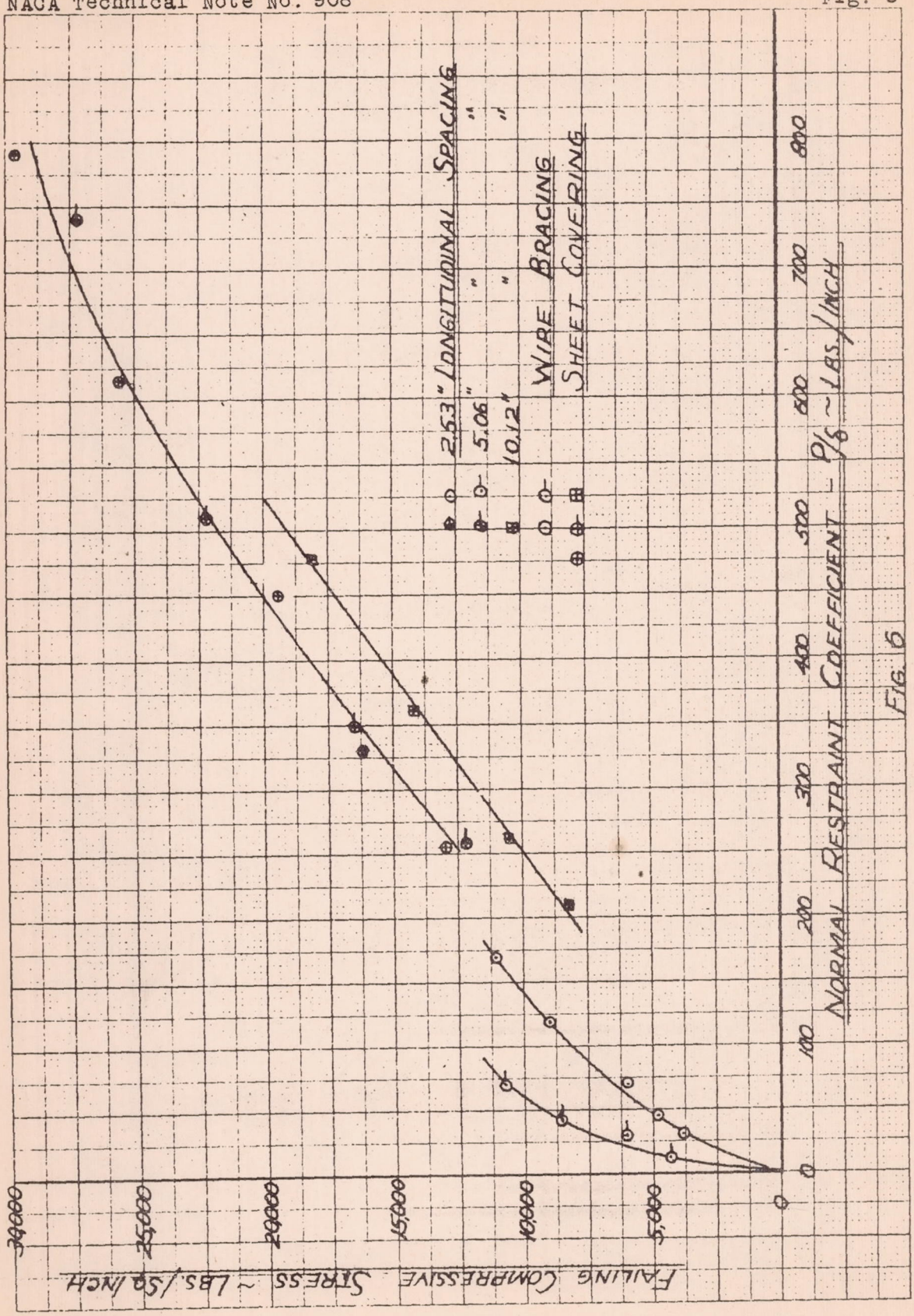
Failing Compressive Stress ~ Lbs./Sq.Inch
30000
25000
20000
15000
10000
5000
0
0
100
200
300
400
500
600
700
800
Normal Restraint Coefficient - P/δ ~ Lbs./Inch
2.53" Longitudinal Spacing
5.06" " "
10.12" " "
Wire Bracing
Sheet Covering

Fig. 6

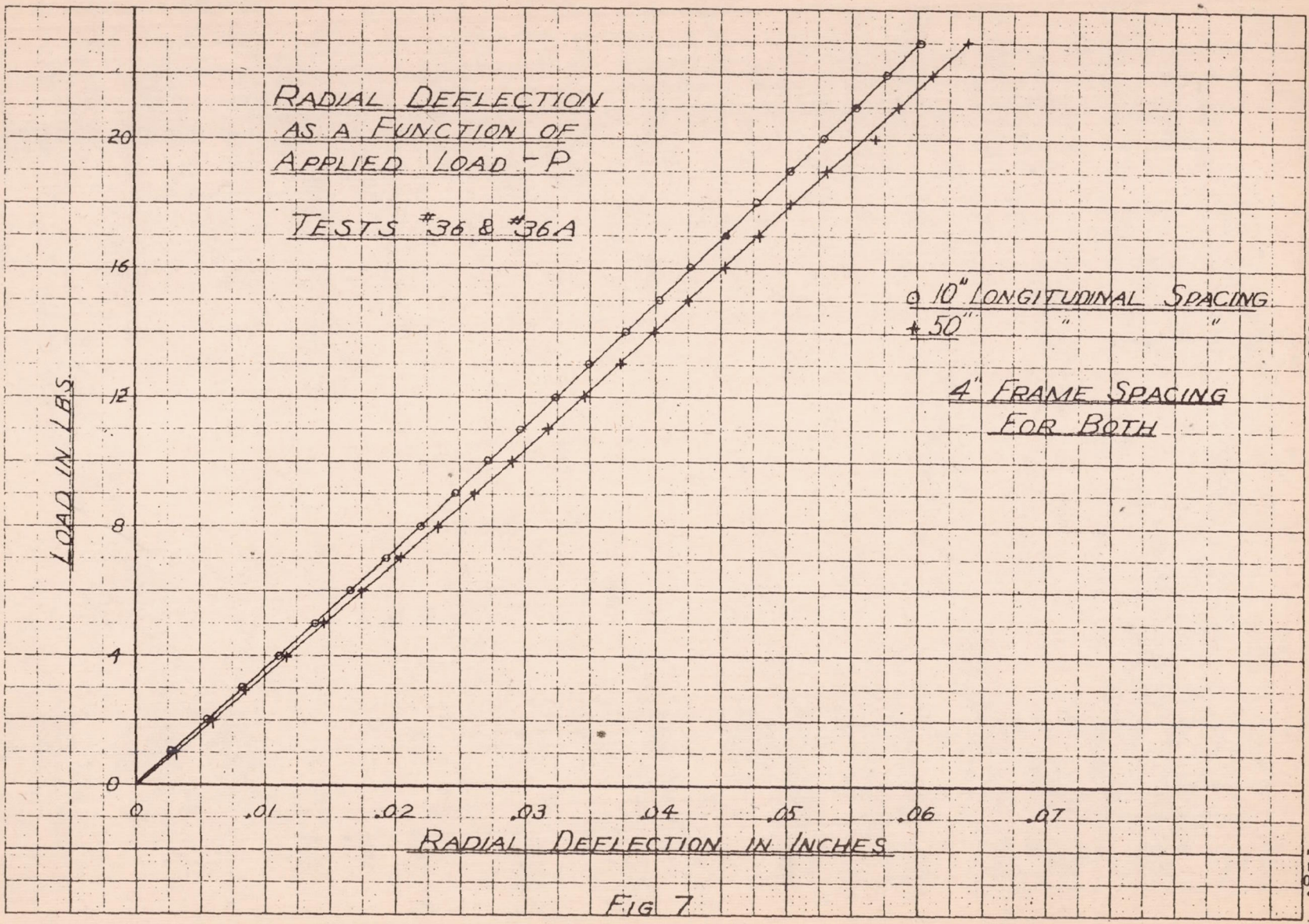
RADIAL DEFLECTION
AS A FUNCTION OF
APPLIED LOAD - P
TESTS #36 & #36A
○ 10" LONGITUDINAL SPACING
★ 50" " "
4" FRAME SPACING
FOR BOTH
LOAD IN LBS.
0
4
8
12
16
20
0
.01
.02
.03
.04
.05
.06
.07
RADIAL DEFLECTION IN INCHES

FIG 7

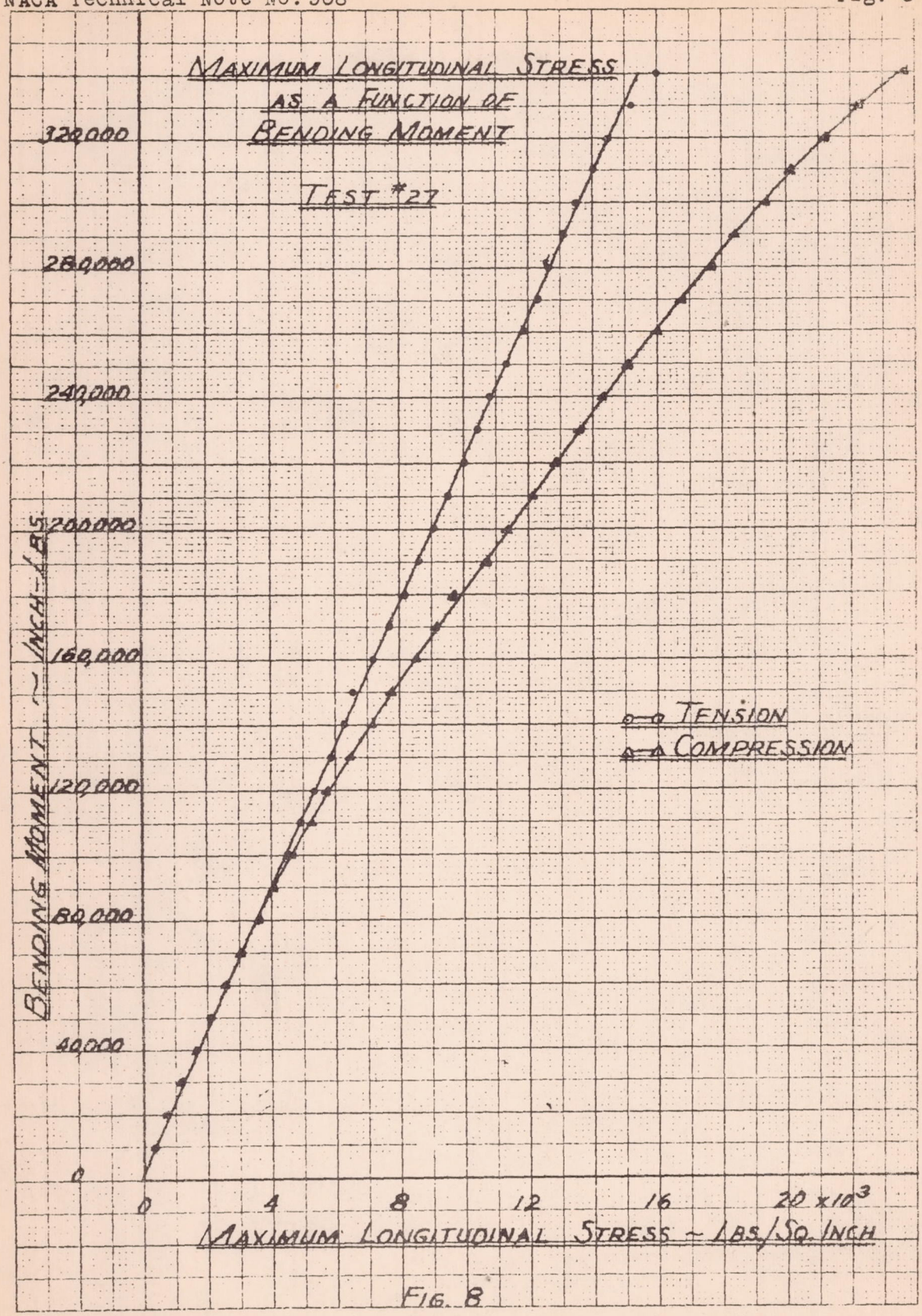
MAXIMUM LONGITUDINAL STRESS
AS A FUNCTION OF
BENDING MOMENT
TEST #27
320,000
280,000
240,000
200,000
160,000
120,000
80,000
40,000
0
BENDING MOMENT ~ INCH-LBS
0
4
8
12
16
20 x10³
MAXIMUM LONGITUDINAL STRESS ~ LBS/SQ. INCH
o—o TENSION
Δ—Δ COMPRESSION

FIG. 8

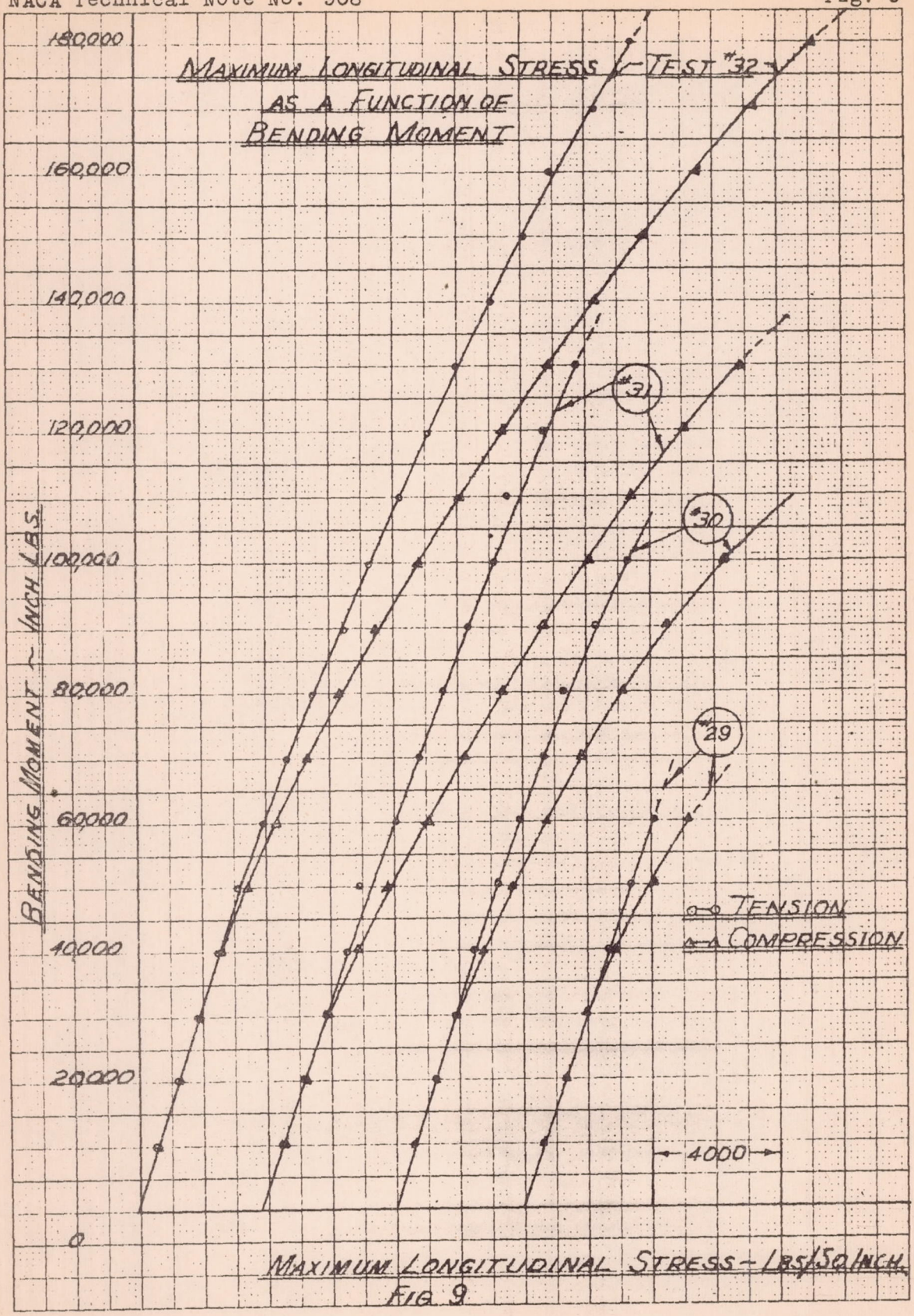
MAXIMUM LONGITUDINAL STRESS - TEST #32
AS A FUNCTION OF
BENDING MOMENT
180,000
160,000
140,000
120,000
100,000
80,000
60,000
40,000
20,000
0
BENDING MOMENT - INCH LBS.
#31
#30
#29
TENSION
COMPRESSION
4000
MAXIMUM LONGITUDINAL STRESS - LBS/SQ INCH.

FIG. 9

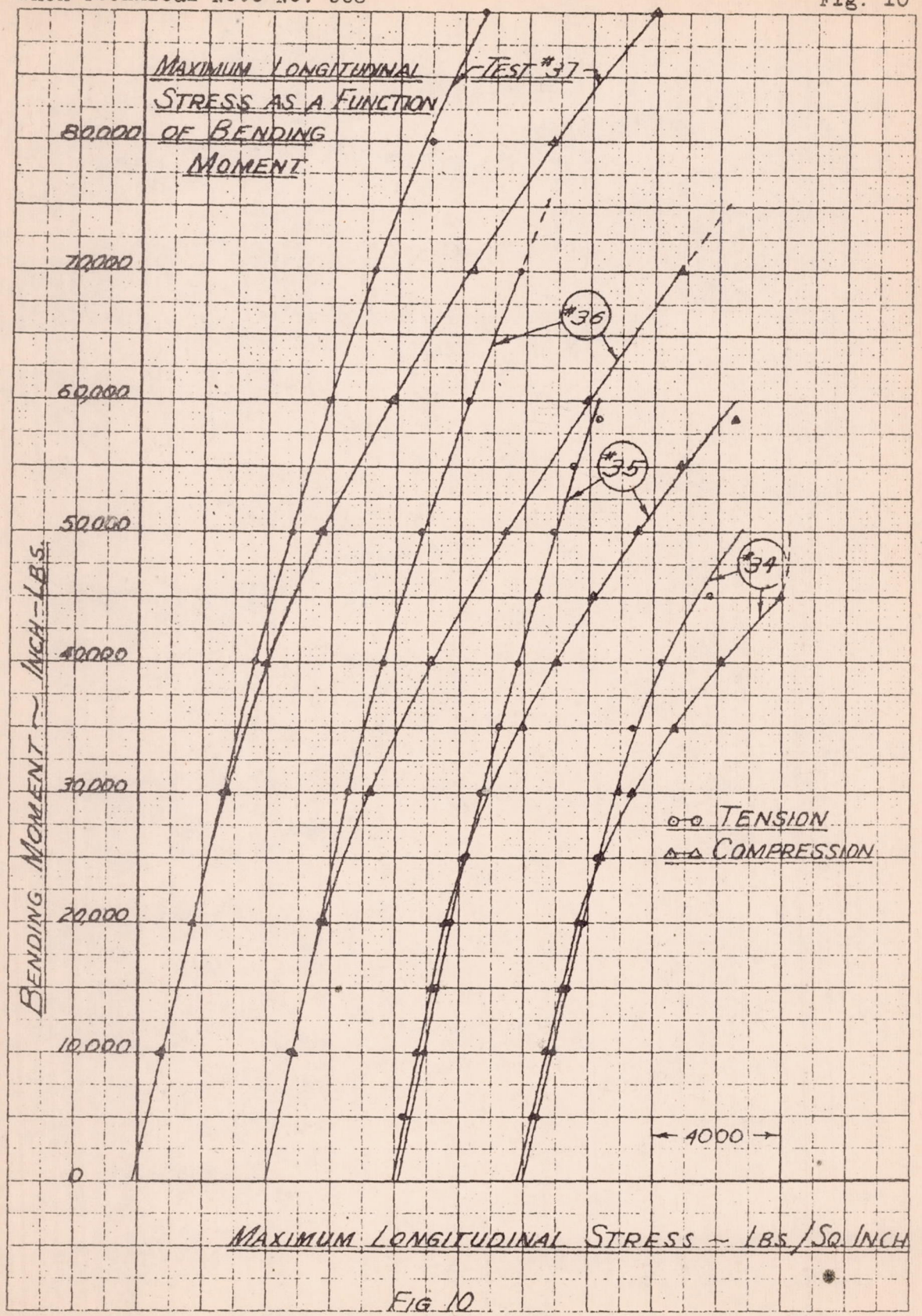
MAXIMUM LONGITUDINAL STRESS AS A FUNCTION OF BENDING MOMENT
TEST #37
#36
#35
#34
80,000
70,000
60,000
50,000
40,000
30,000
20,000
10,000
0
BENDING MOMENT ~ INCH-LBS.
TENSION
COMPRESSION
4000
MAXIMUM LONGITUDINAL STRESS ~ LBS./SQ INCH

FIG 10

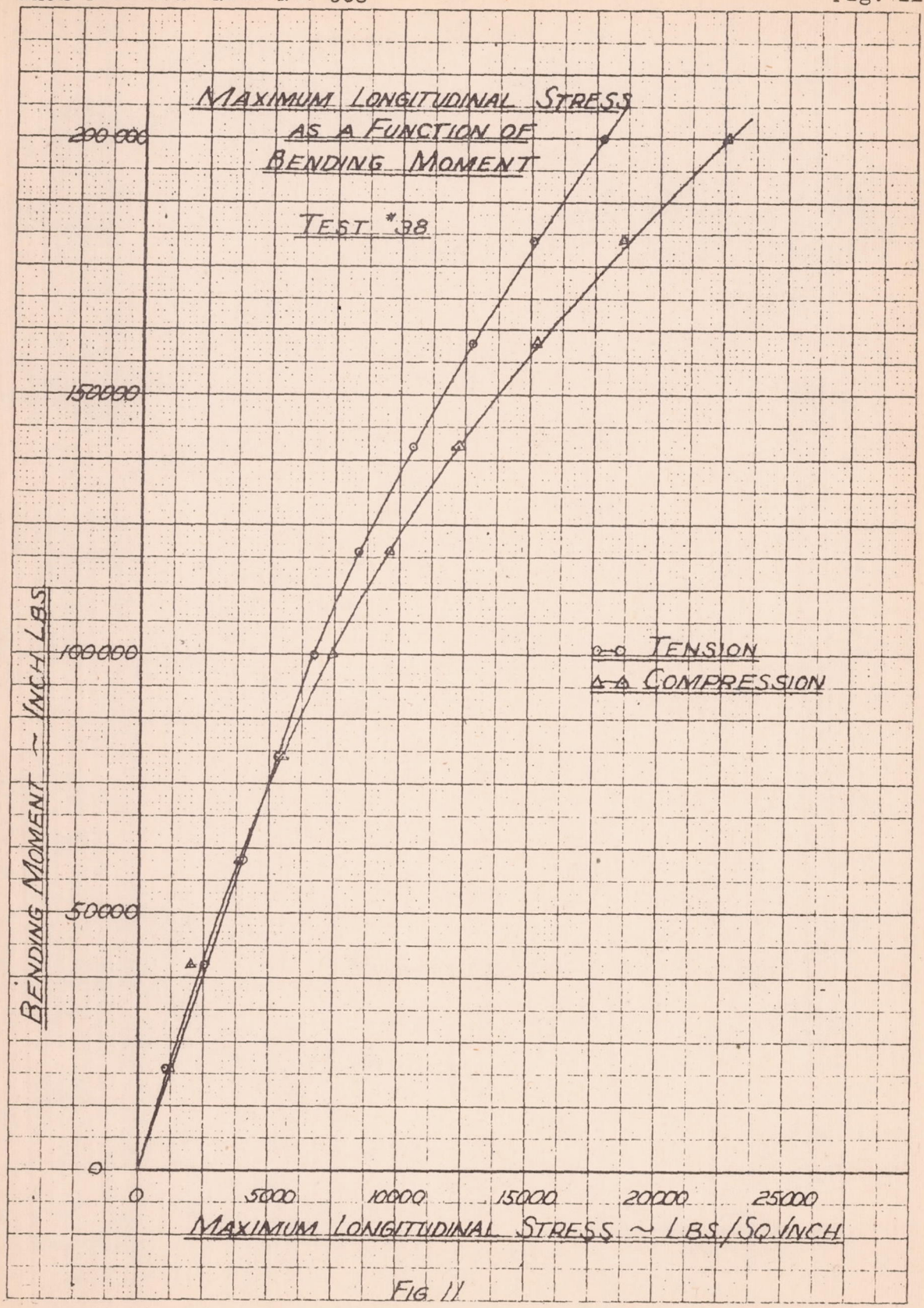
MAXIMUM LONGITUDINAL STRESS
AS A FUNCTION OF
BENDING MOMENT
TEST *38
200000
150000
100000
50000
0
BENDING MOMENT ~ INCH LBS
o—o TENSION
Δ—Δ COMPRESSION
0
5000
10000
15000
20000
25000
MAXIMUM LONGITUDINAL STRESS ~ LBS./SQ.INCH

FIG. 11

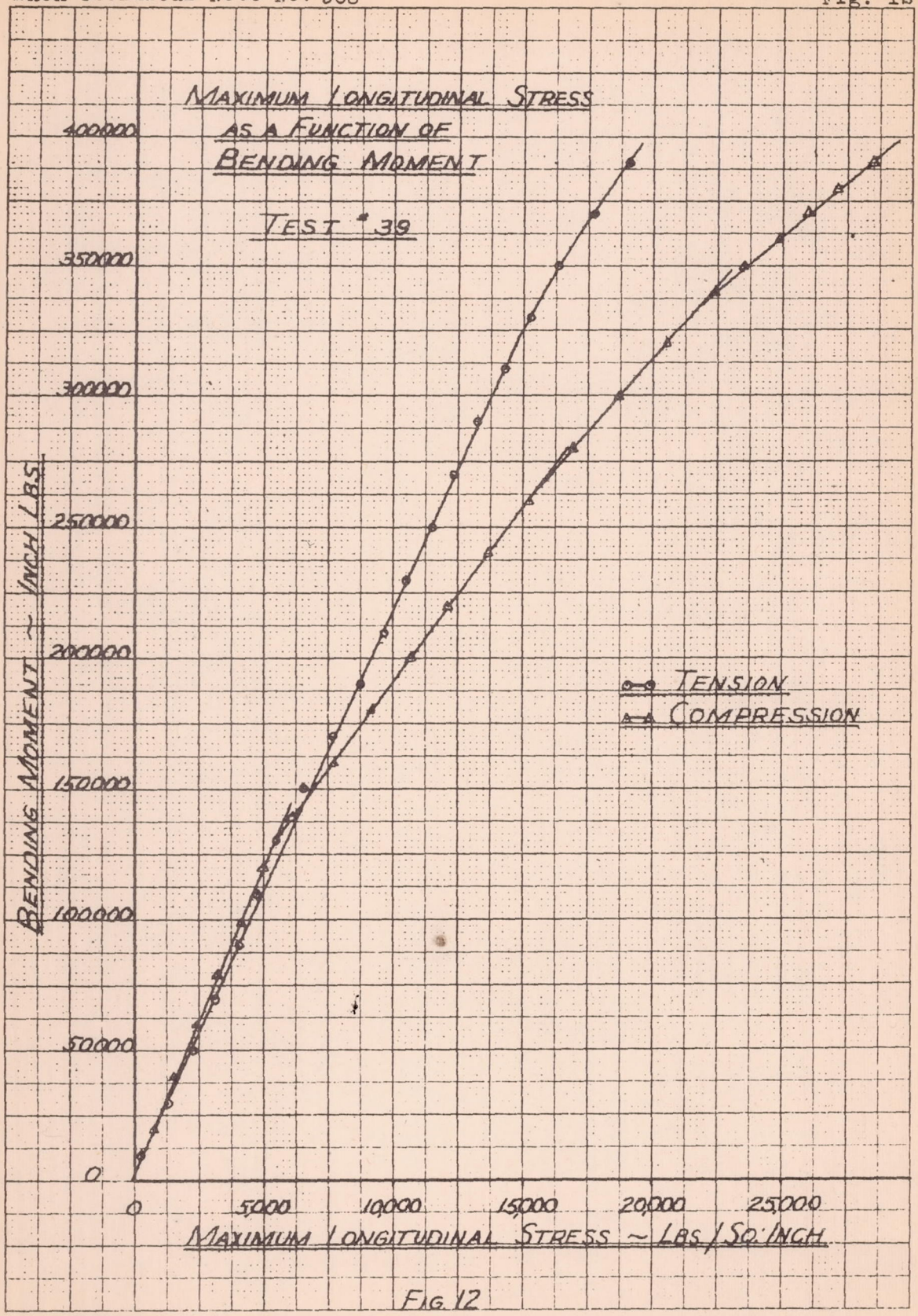
MAXIMUM LONGITUDINAL STRESS
AS A FUNCTION OF
BENDING MOMENT
TEST #39
BENDING MOMENT ~ INCH LBS.
400000
350000
300000
250000
200000
150000
100000
50000
0
0
5,000
10,000
15,000
20,000
25,000
MAXIMUM LONGITUDINAL STRESS ~ LBS / SQ. INCH
TENSION
COMPRESSION

FIG. 12

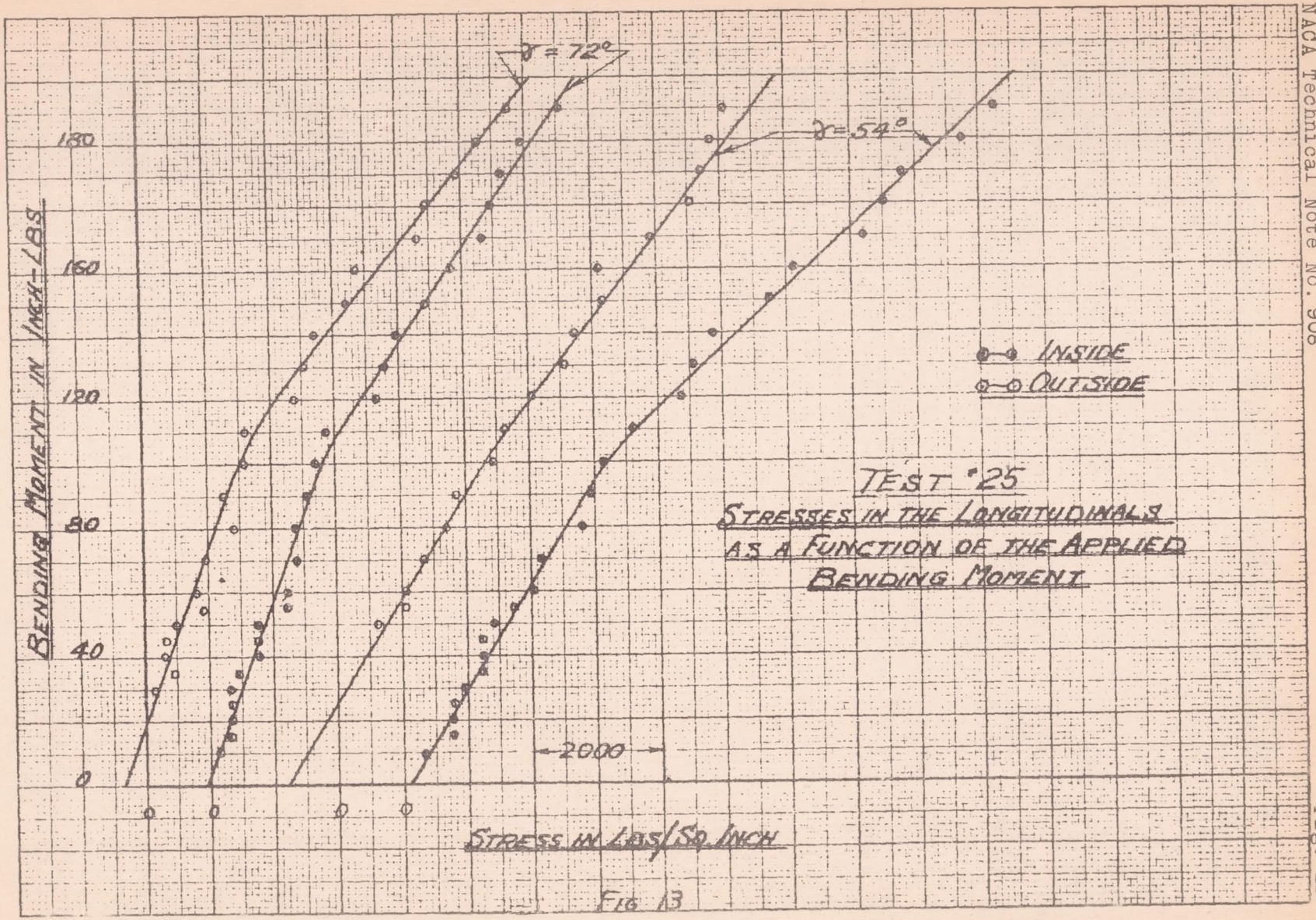
γ = 72°
γ = 54°
180
160
120
80
40
0
2000
BENDING MOMENT IN INCH-LBS
STRESS IN LBS/SQ. INCH
INSIDE
OUTSIDE
TEST 25
STRESSES IN THE LONGITUDINALS
AS A FUNCTION OF THE APPLIED
BENDING MOMENT

FIG 13

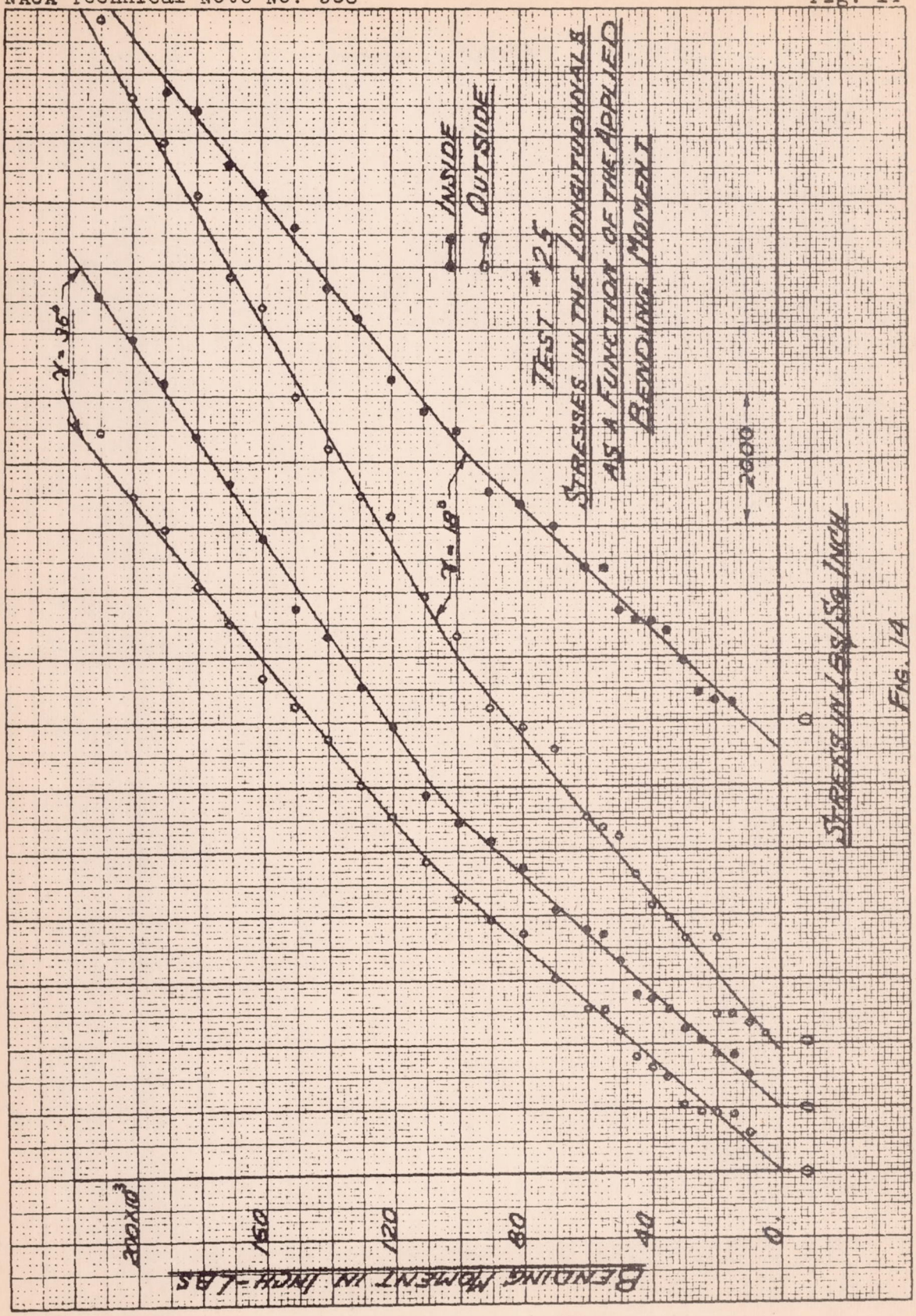
Stresses in the Longitudinals as a Function of the Applied Bending Moment
Test #25
Inside
Outside
γ = 36°
γ = 18°
Bending Moment in Inch-Lbs
200x10³
160
120
80
40
0
2000
0
Stress in Lbs/Sq Inch

Fig. 14

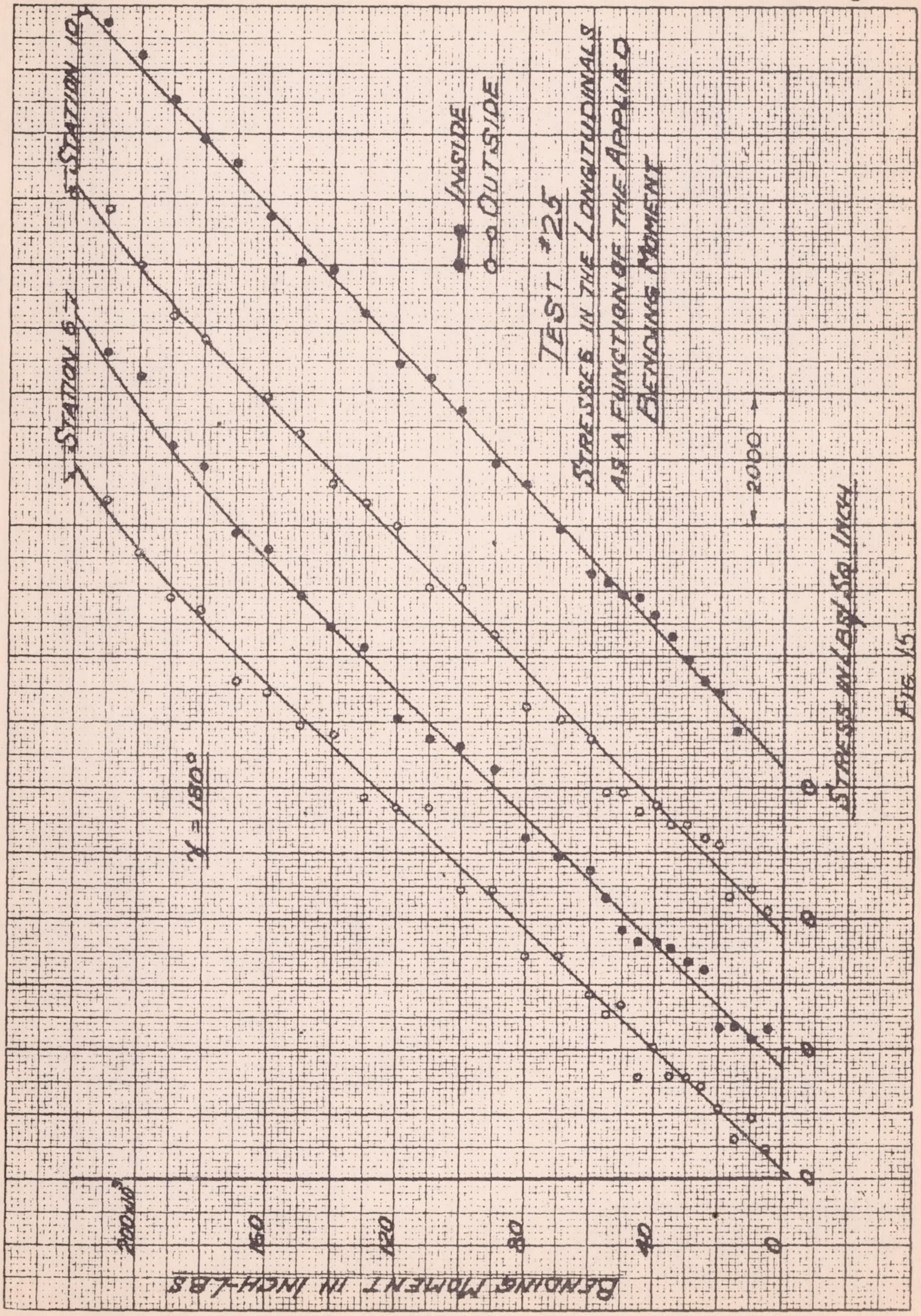
STATION 10
STATION 6
INSIDE
OUTSIDE
TEST #25
STRESSES IN THE LONGITUDINALS
AS A FUNCTION OF THE APPLIED
BENDING MOMENT
γ = 180°
2000
STRESS IN LBS/SQ. INCH
200x10³
160
120
80
40
0
BENDING MOMENT IN INCH-LBS

FIG. 15

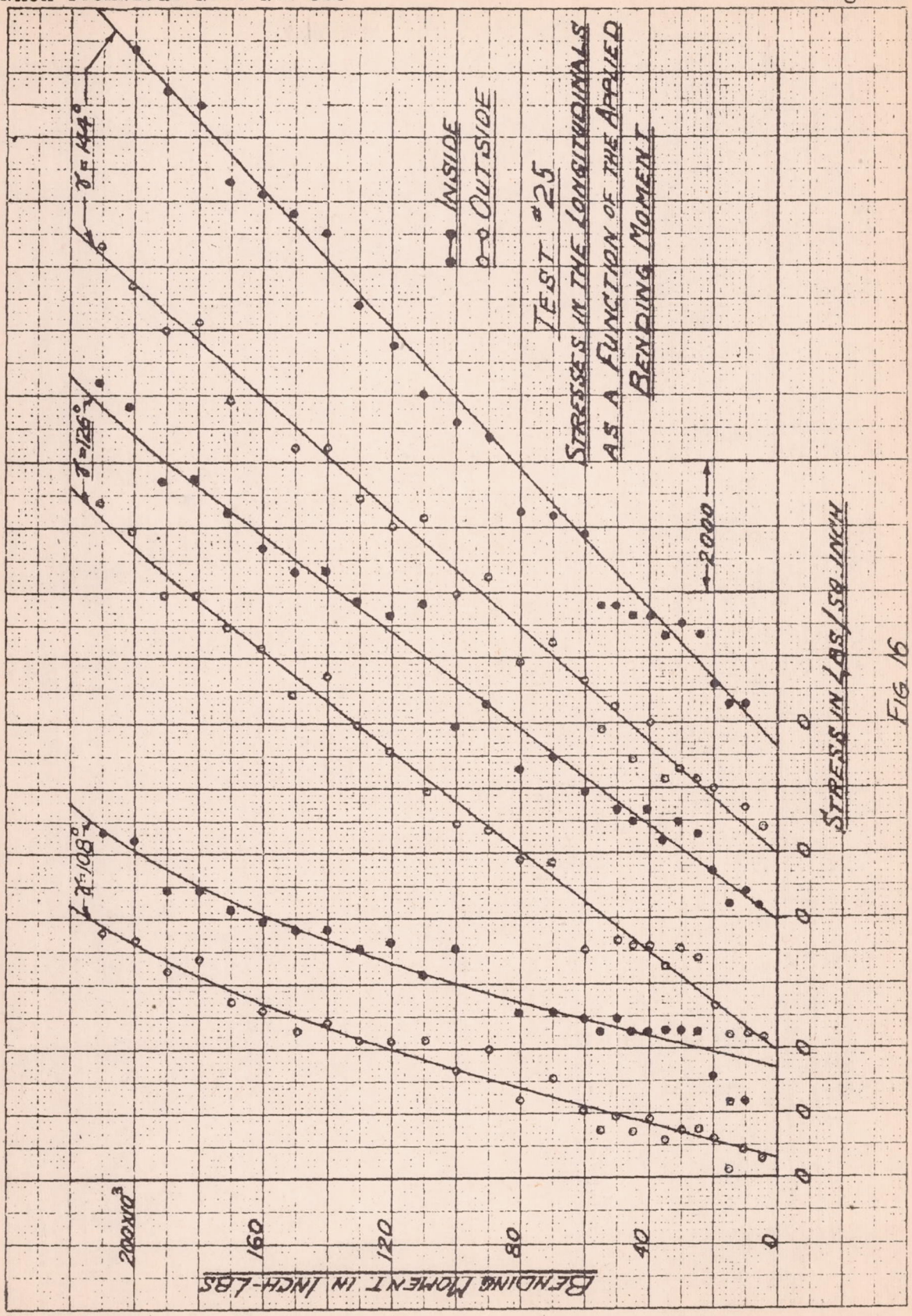
STRESSES IN THE LONGITUDINALS AS A FUNCTION OF THE APPLIED BENDING MOMENT
TEST #25
INSIDE
OUTSIDE
γ = 144°
γ = 126°
γ = 108°
2000
STRESS IN LBS./SQ. INCH
BENDING MOMENT IN INCH-LBS.
200x10³
160
120
80
40
0

FIG 16

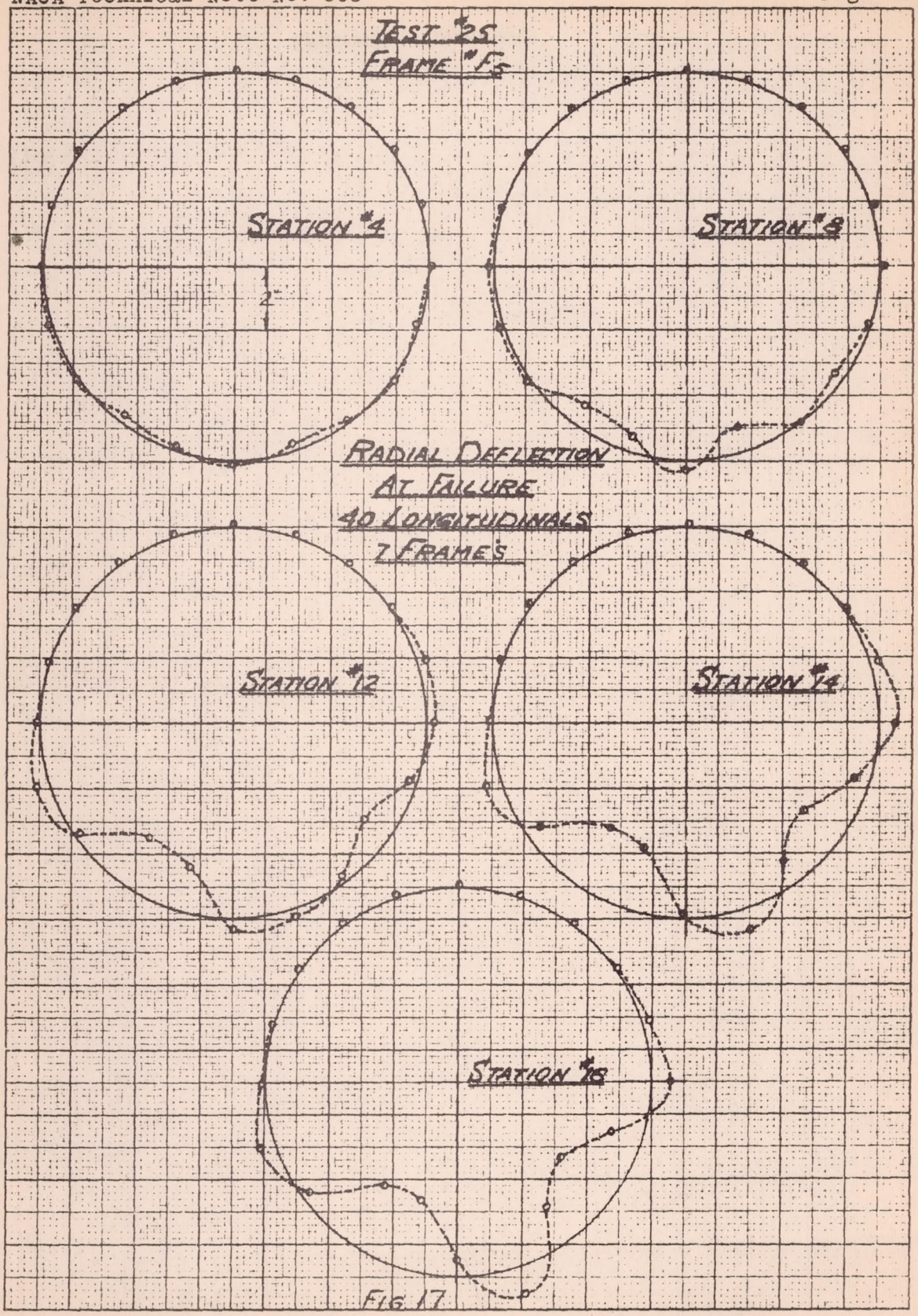
TEST #25
FRAME # F5
STATION #4
STATION #8
1
2
RADIAL DEFLECTION
AT FAILURE
40 LONGITUDINALS
7 FRAME'S
STATION #12
STATION #14
STATION #18

FIG. 17

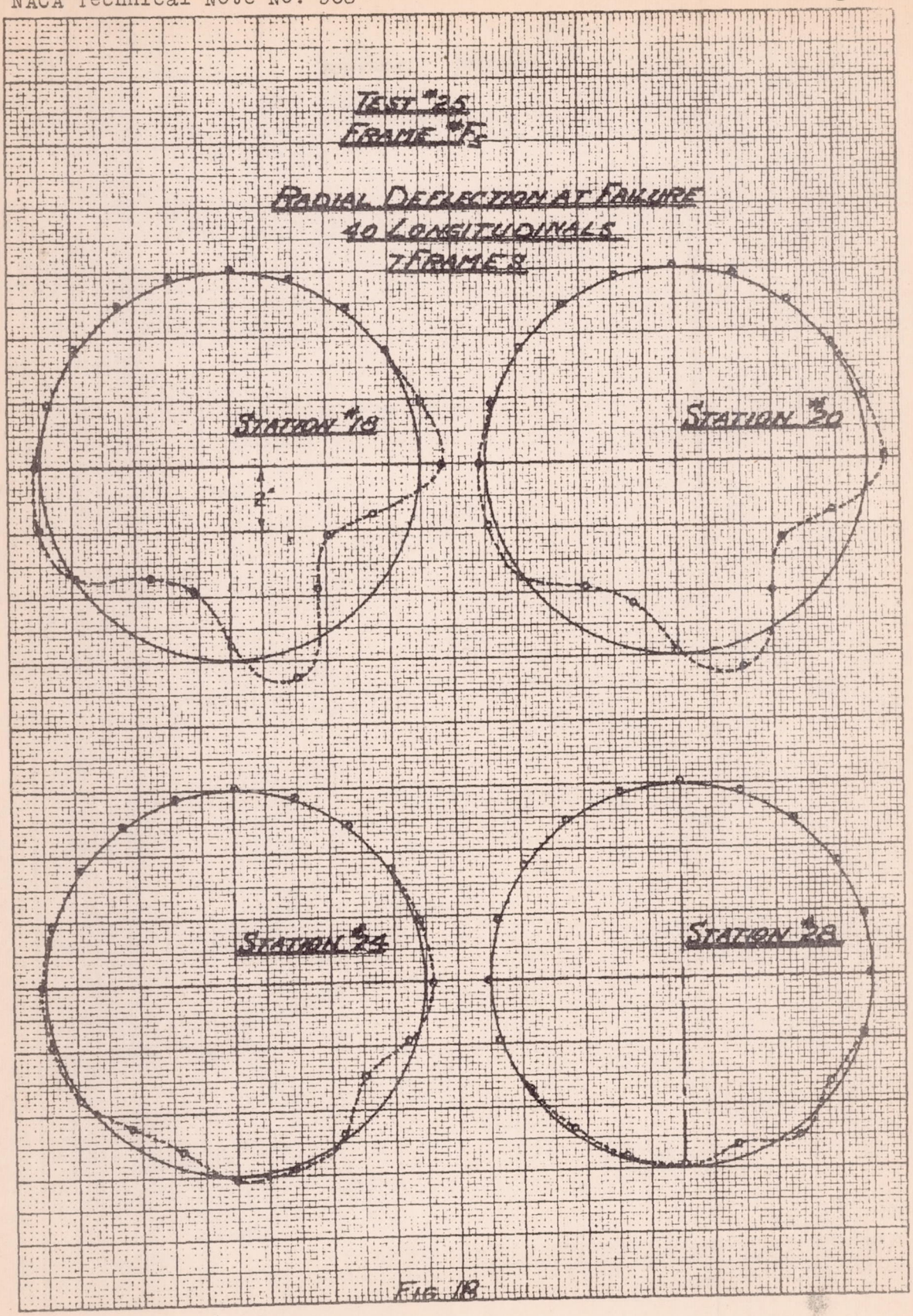
Test #25
Frame #F2
Radial Deflection at Failure
40 Longitudinals
7 Frames
Station #28
2"
Station #30
Station #24
Station #32

Fig. 18

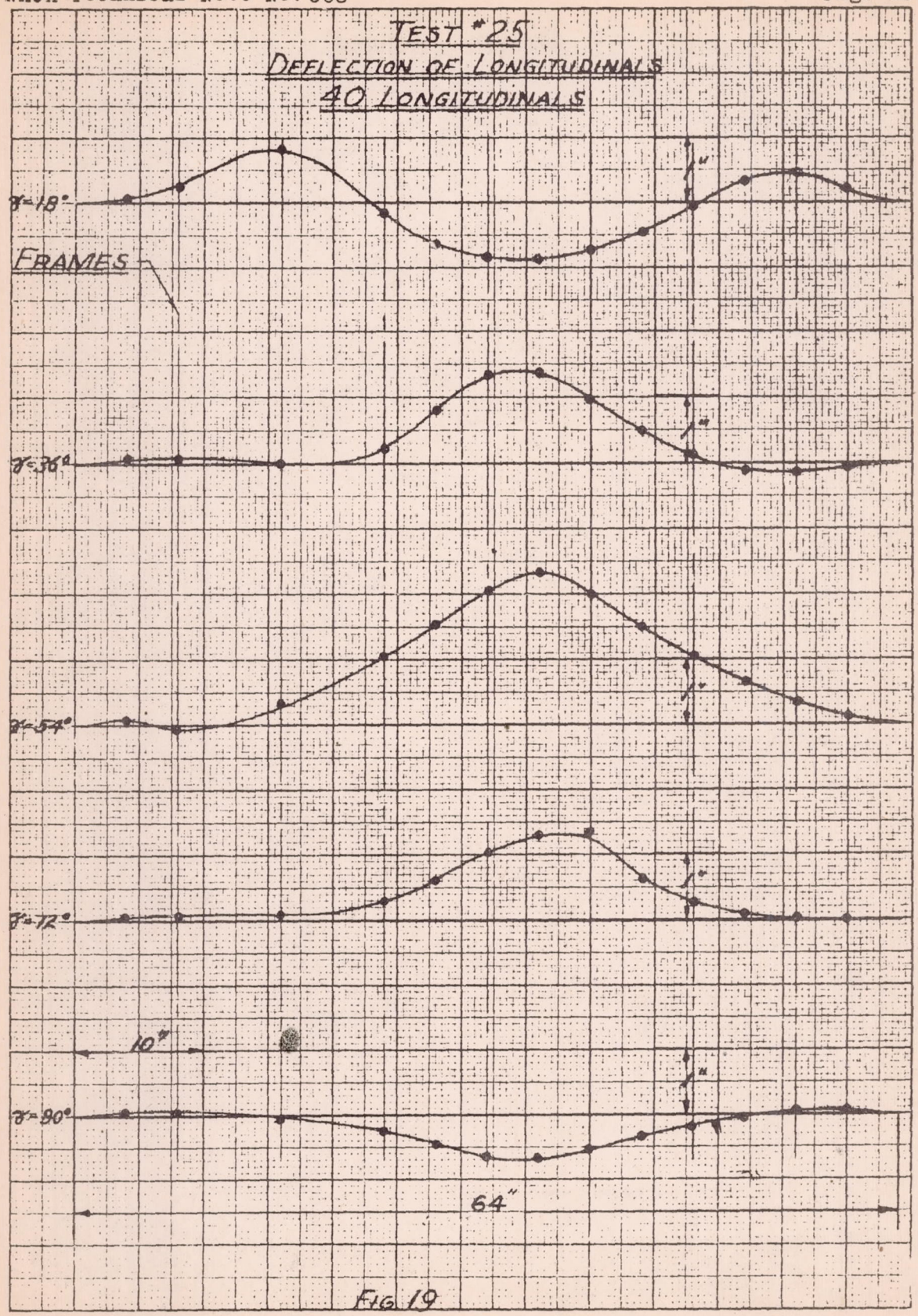
TEST #25
DEFLECTION OF LONGITUDINALS
40 LONGITUDINALS
γ=18°
FRAMES
γ=36°
γ=54°
γ=72°
10"
γ=90°
64"

FIG 19

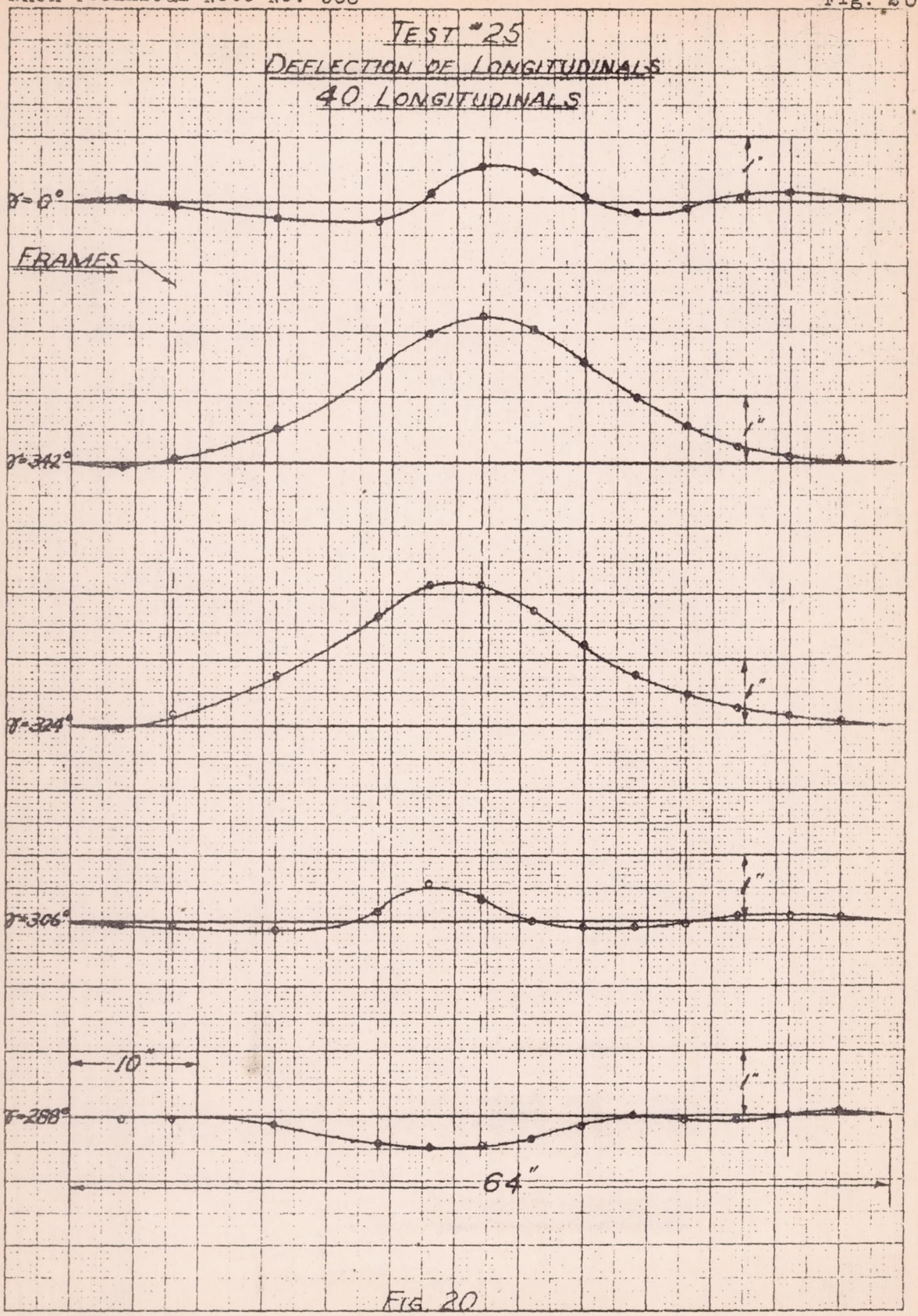
TEST #25
DEFLECTION OF LONGITUDINALS
40 LONGITUDINALS
γ=0°
FRAMES
γ=342°
γ=324°
γ=306°
γ=288°
1"
10"
64"

FIG. 20

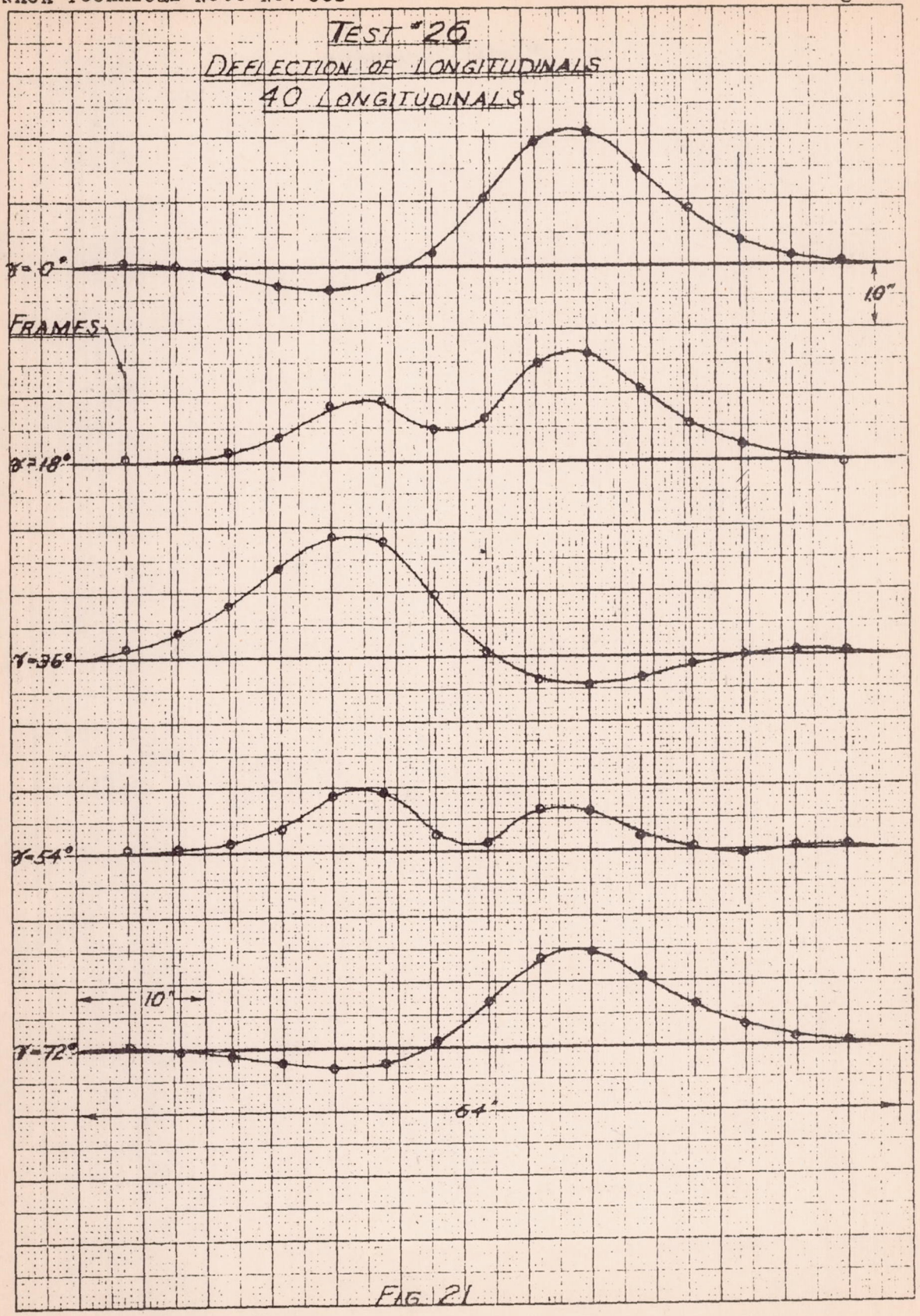
TEST "26
DEFLECTION OF LONGITUDINALS
40 LONGITUDINALS
γ=0°
10"
FRAMES
γ=18°
γ=36°
γ=54°
10"
γ=72°
64"

FIG. 21

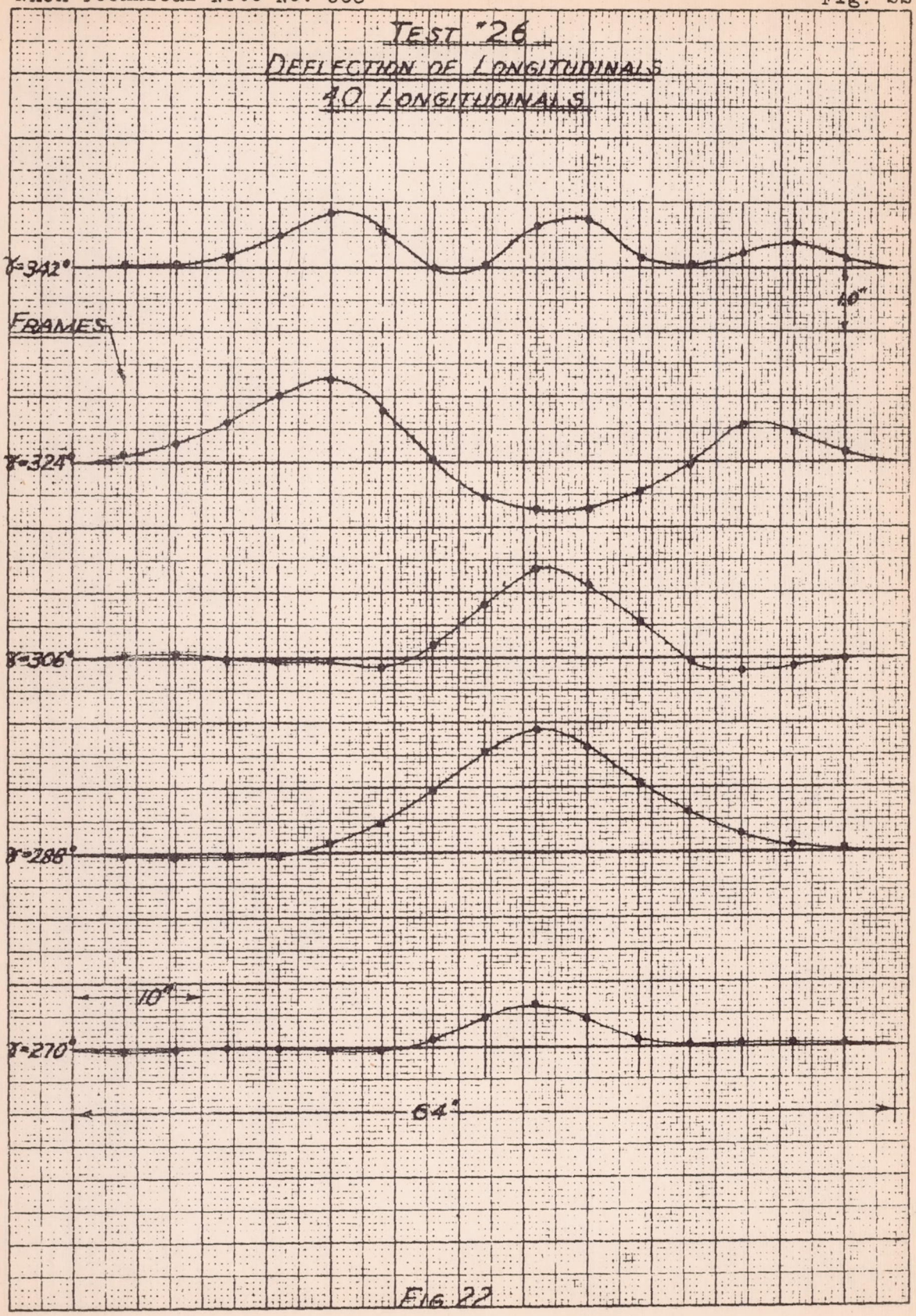
TEST "26"
DEFLECTION OF LONGITUDINALS
40 LONGITUDINALS
γ=342°
10"
FRAMES
γ=324°
γ=306°
γ=288°
10"
γ=270°
64"

Fig. 22

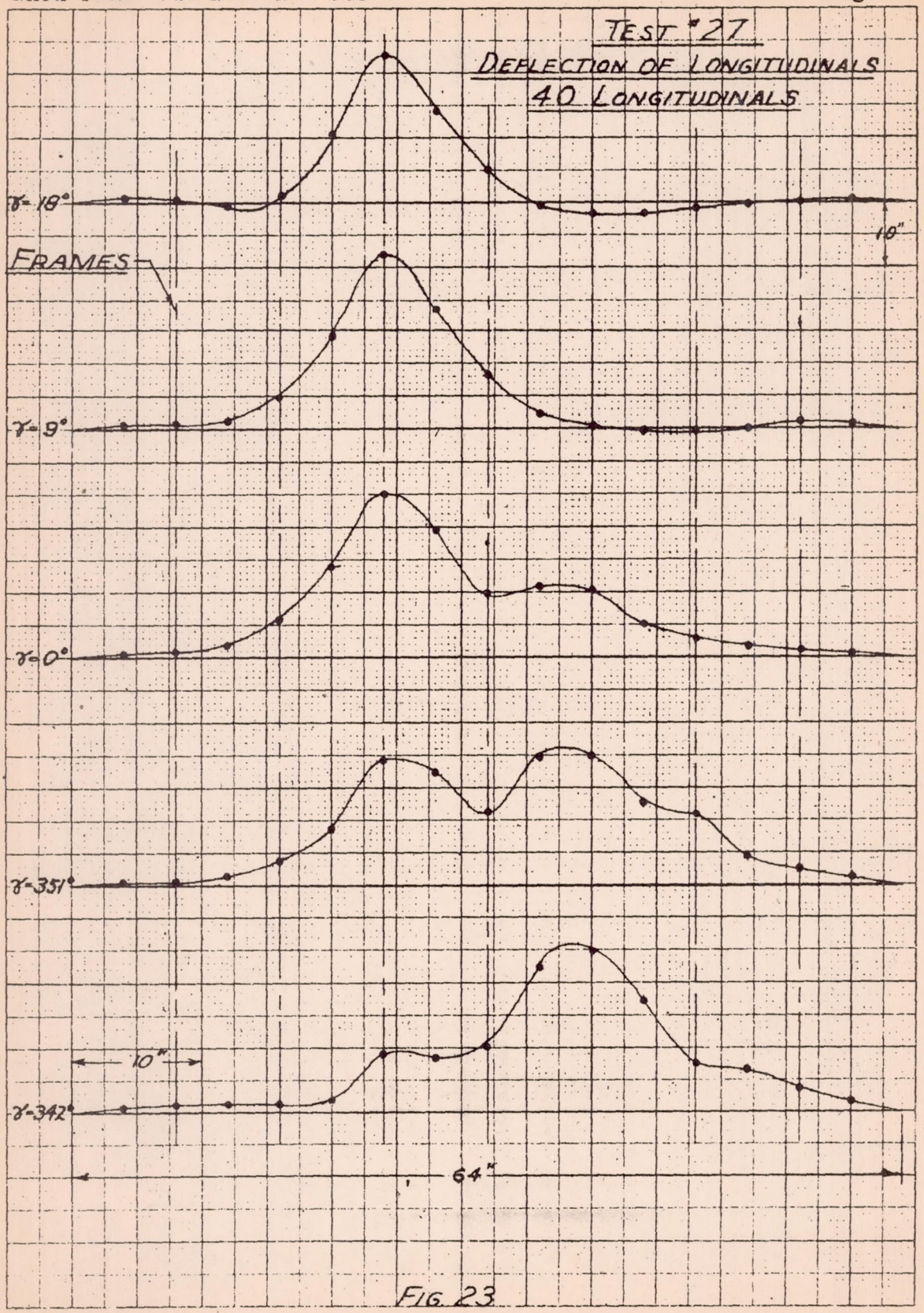
TEST #27
DEFLECTION OF LONGITUDINALS
40 LONGITUDINALS
γ-18°
10"
FRAMES
γ-9°
γ-0°
γ-351°
10"
γ-342°
64"

FIG. 23

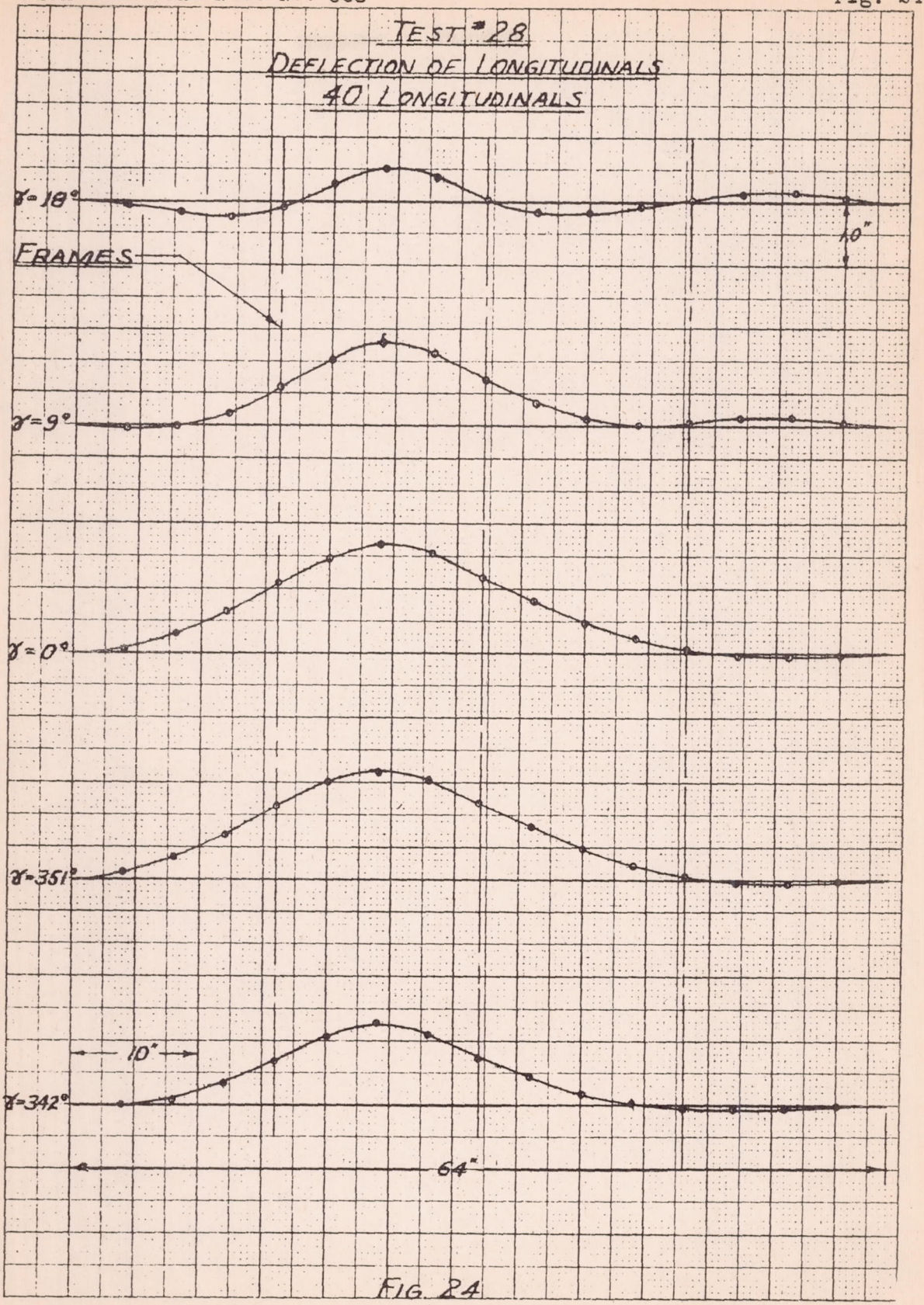
TEST #28
DEFLECTION OF LONGITUDINALS
40 LONGITUDINALS
γ=18°
FRAMES
1.0"
γ=9°
γ=0°
γ=351°
10"
γ=342°
64"

FIG. 24

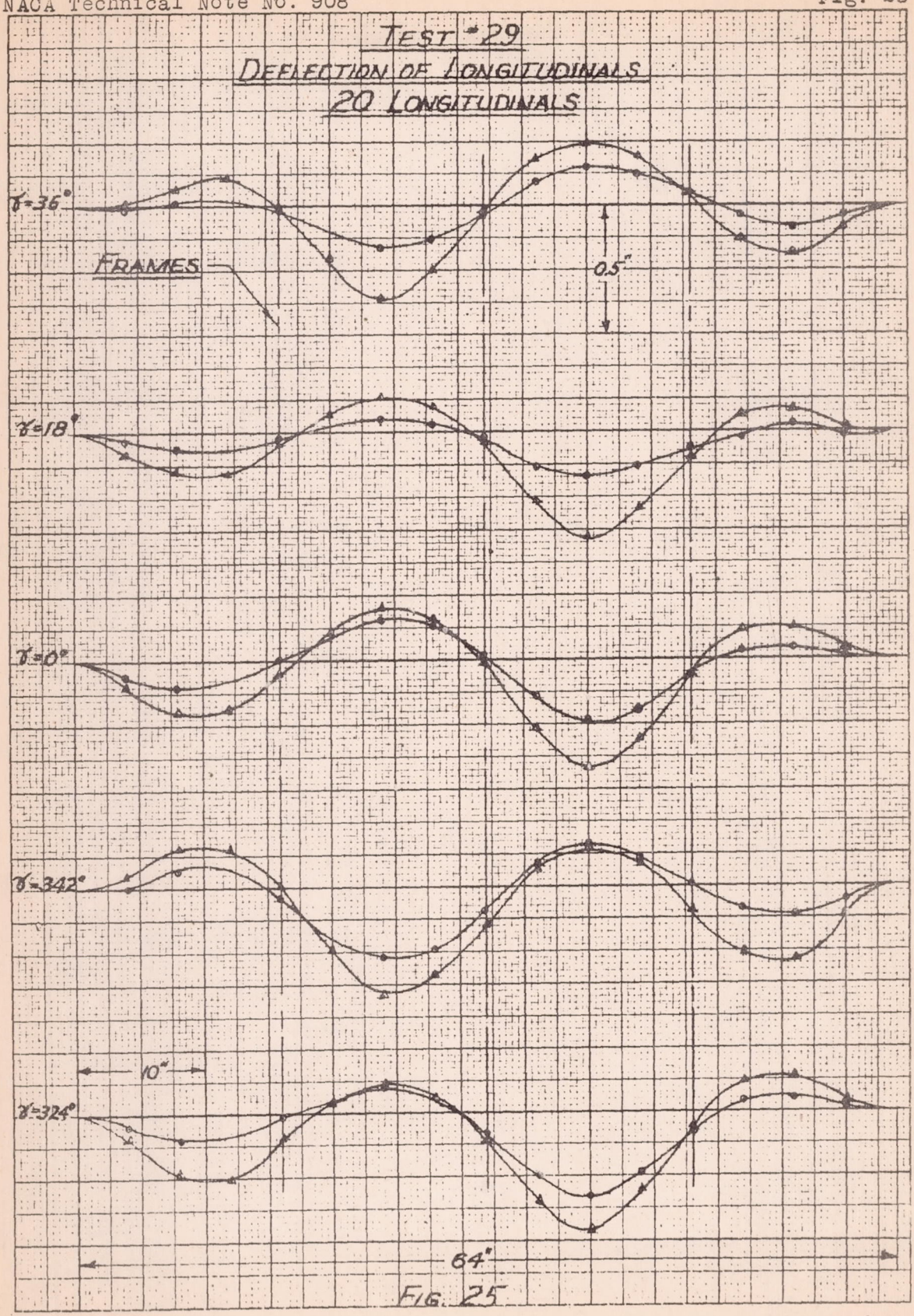
TEST - 29
DEFLECTION OF LONGITUDINALS
20 LONGITUDINALS
γ=36°
FRAMES
0.5"
γ=18°
γ=0°
γ=342°
10"
γ=324°
64"

FIG. 25

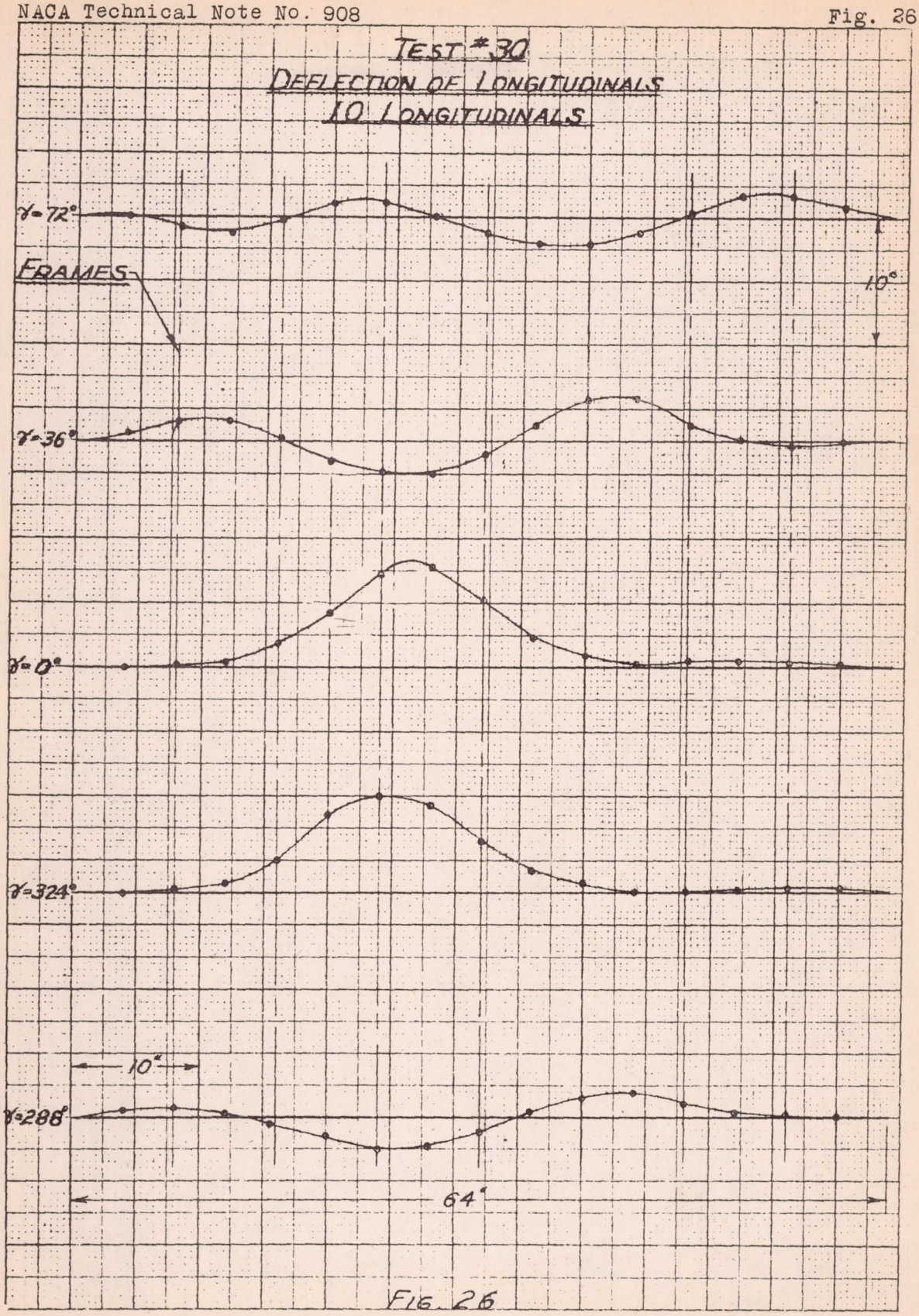
TEST #30
DEFLECTION OF LONGITUDINALS
10 LONGITUDINALS
γ=72°
FRAMES
1.0"
γ=36°
γ=0°
γ=324°
10"
γ=288°
64"

FIG. 26

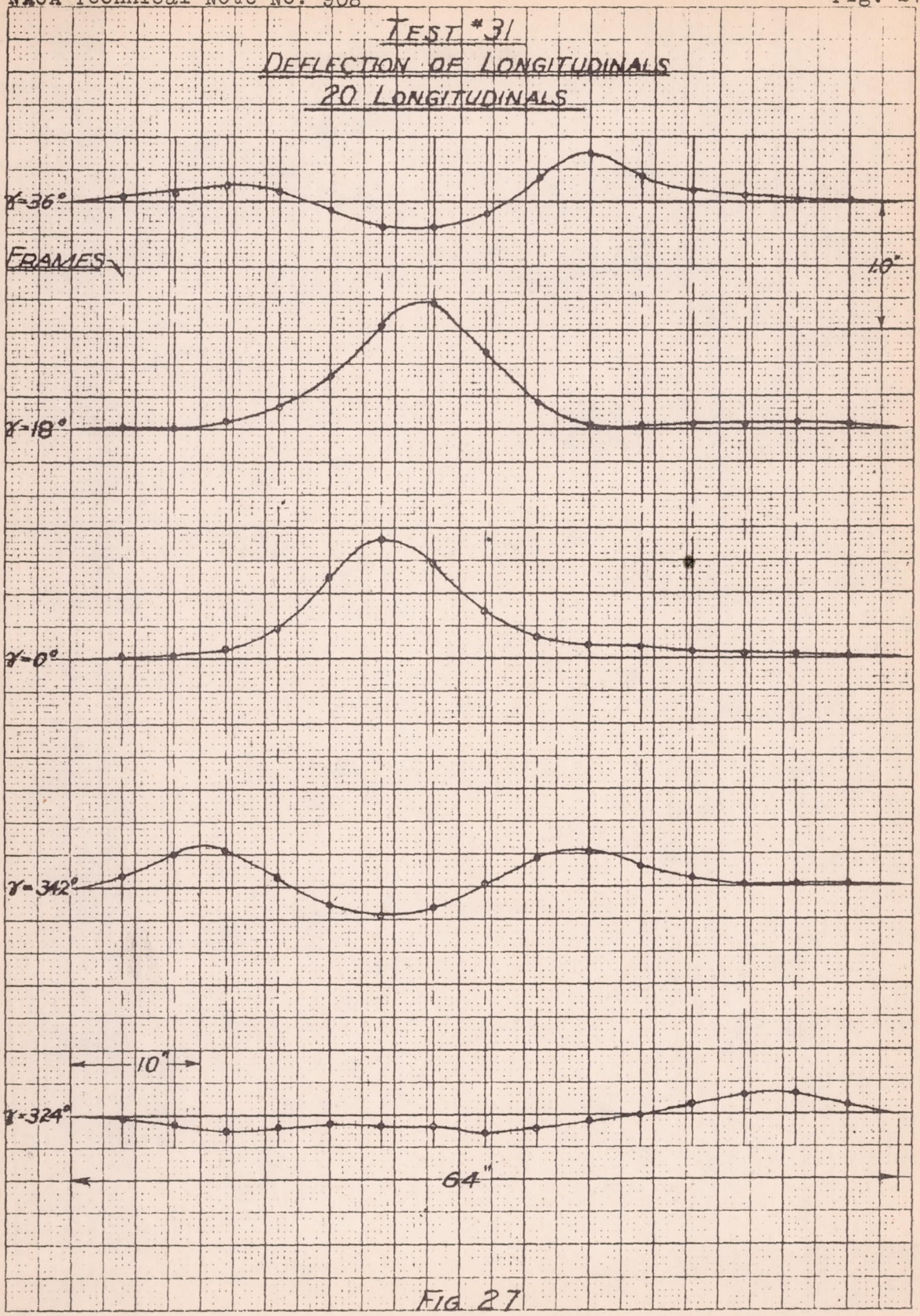
TEST #31
DEFLECTION OF LONGITUDINALS
20 LONGITUDINALS
γ=36°
FRAMES
10"
γ=18°
γ=0°
γ=342°
10"
γ=324°
64"

Fig 27

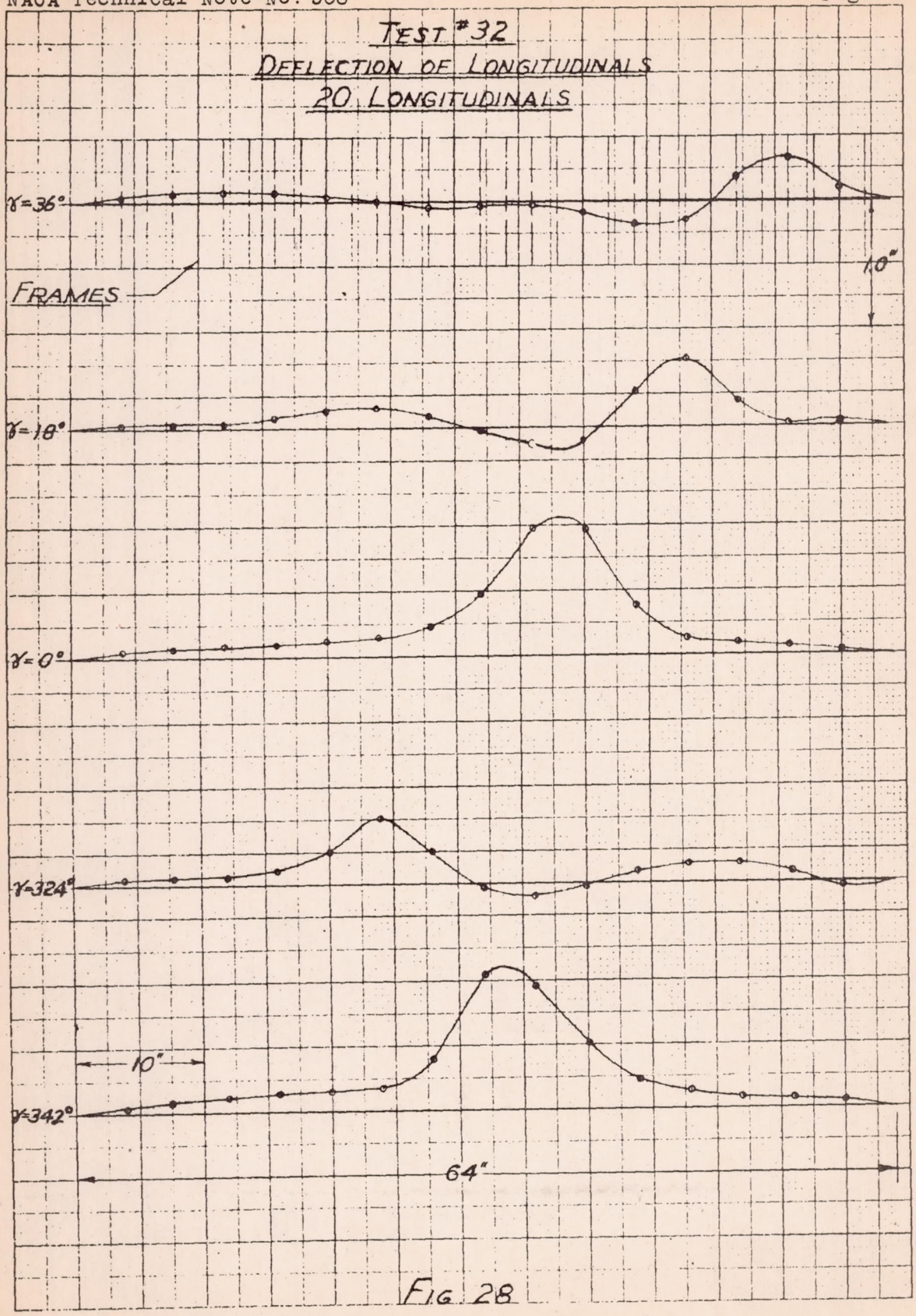
TEST #32
DEFLECTION OF LONGITUDINALS
20 LONGITUDINALS
γ=36°
1.0"
FRAMES
γ=18°
γ=0°
γ=324°
10"
γ=342°
64"

FIG. 28

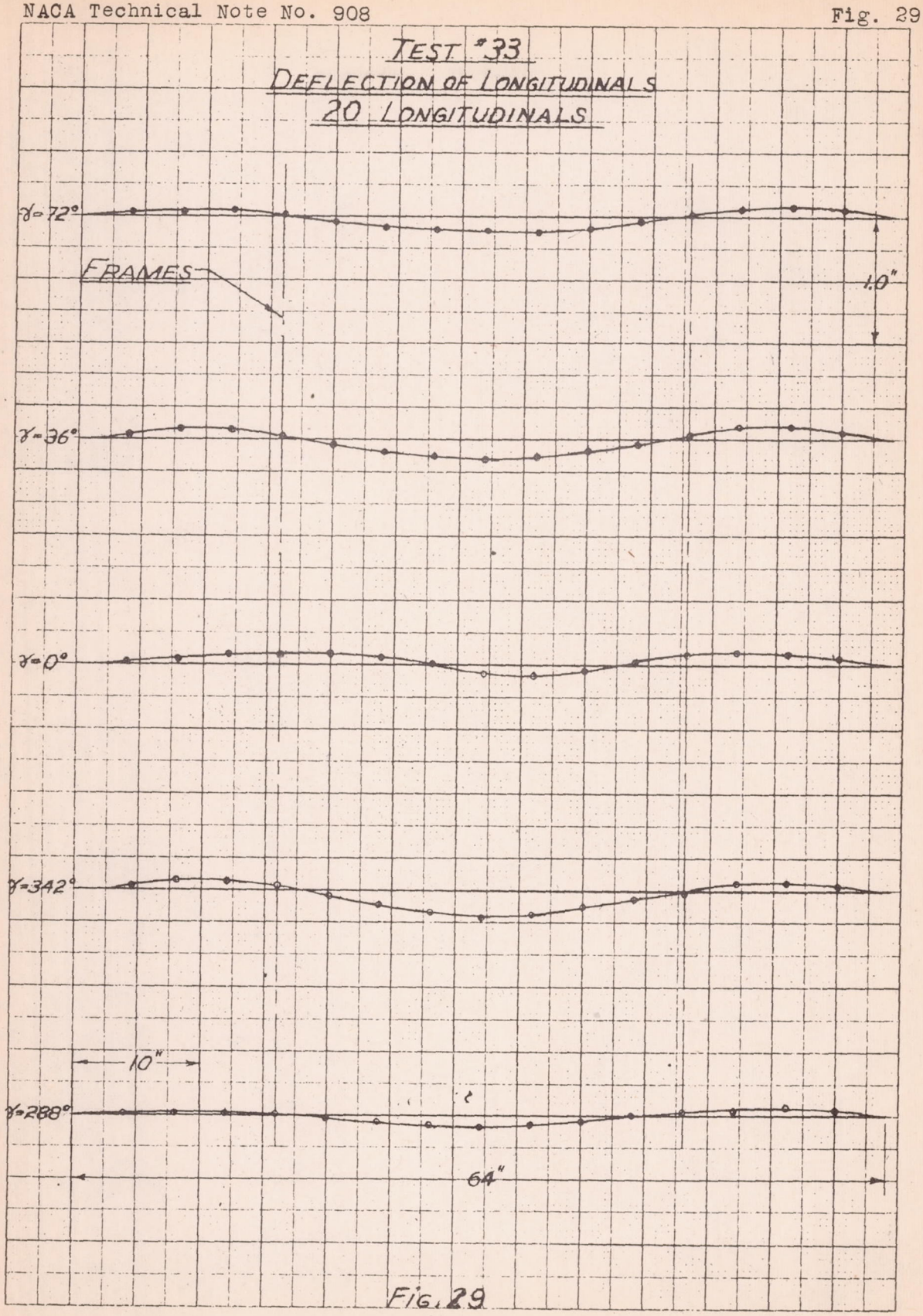
TEST #33
DEFLECTION OF LONGITUDINALS
20 LONGITUDINALS
γ=72°
FRAMES
1.0"
γ=36°
γ=0°
γ=342°
10"
γ=288°
64"

Fig. 29

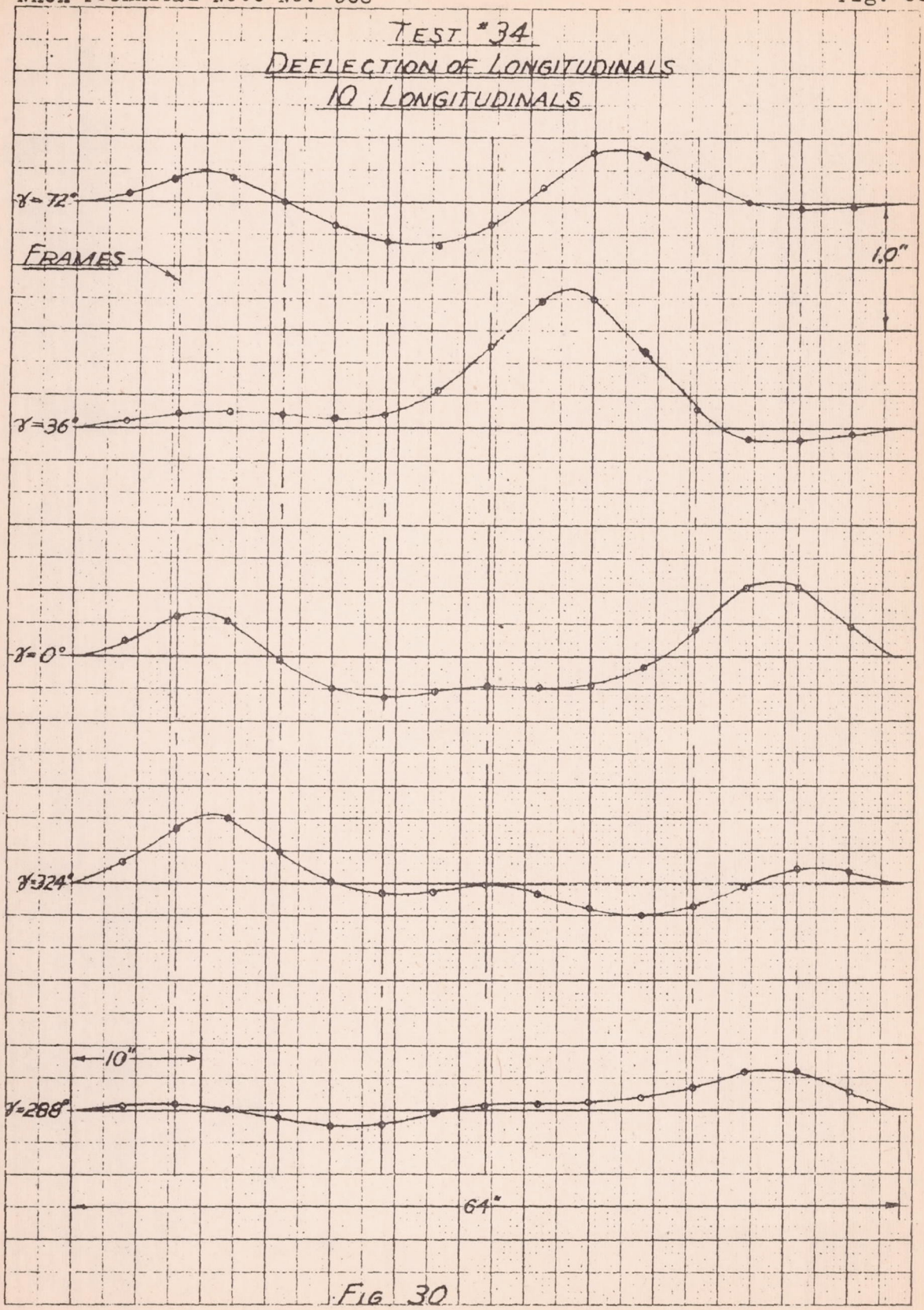
TEST #34
DEFLECTION OF LONGITUDINALS
10 LONGITUDINALS
γ=72°
FRAMES
1.0"
γ=36°
γ=0°
γ=324°
10"
γ=288°
64"

FIG 30

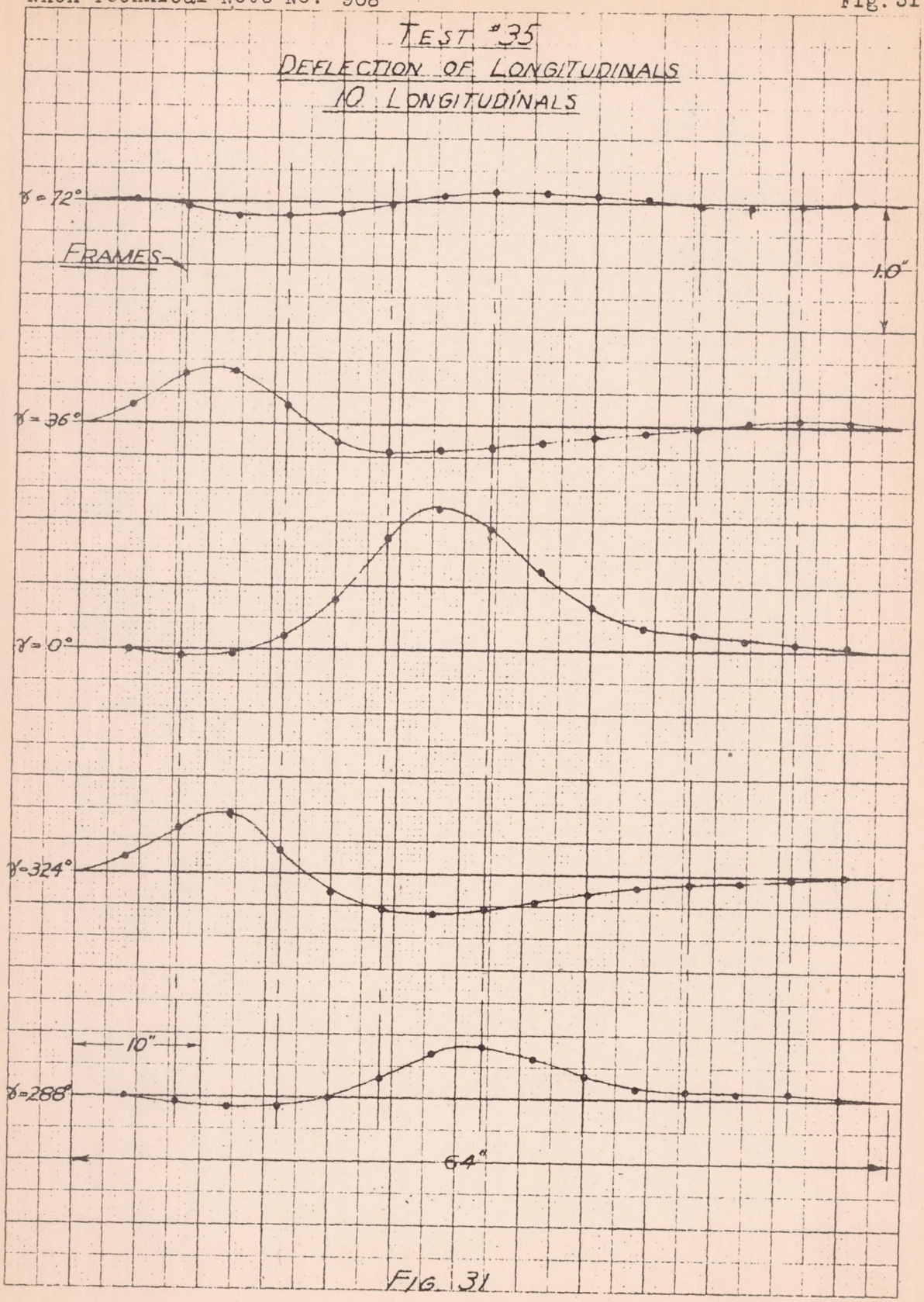
TEST #35
DEFLECTION OF LONGITUDINALS
10 LONGITUDINALS
γ = 72°
FRAMES
1.0"
γ = 36°
γ = 0°
γ = 324°
10"
γ = 288°
64"

FIG. 31

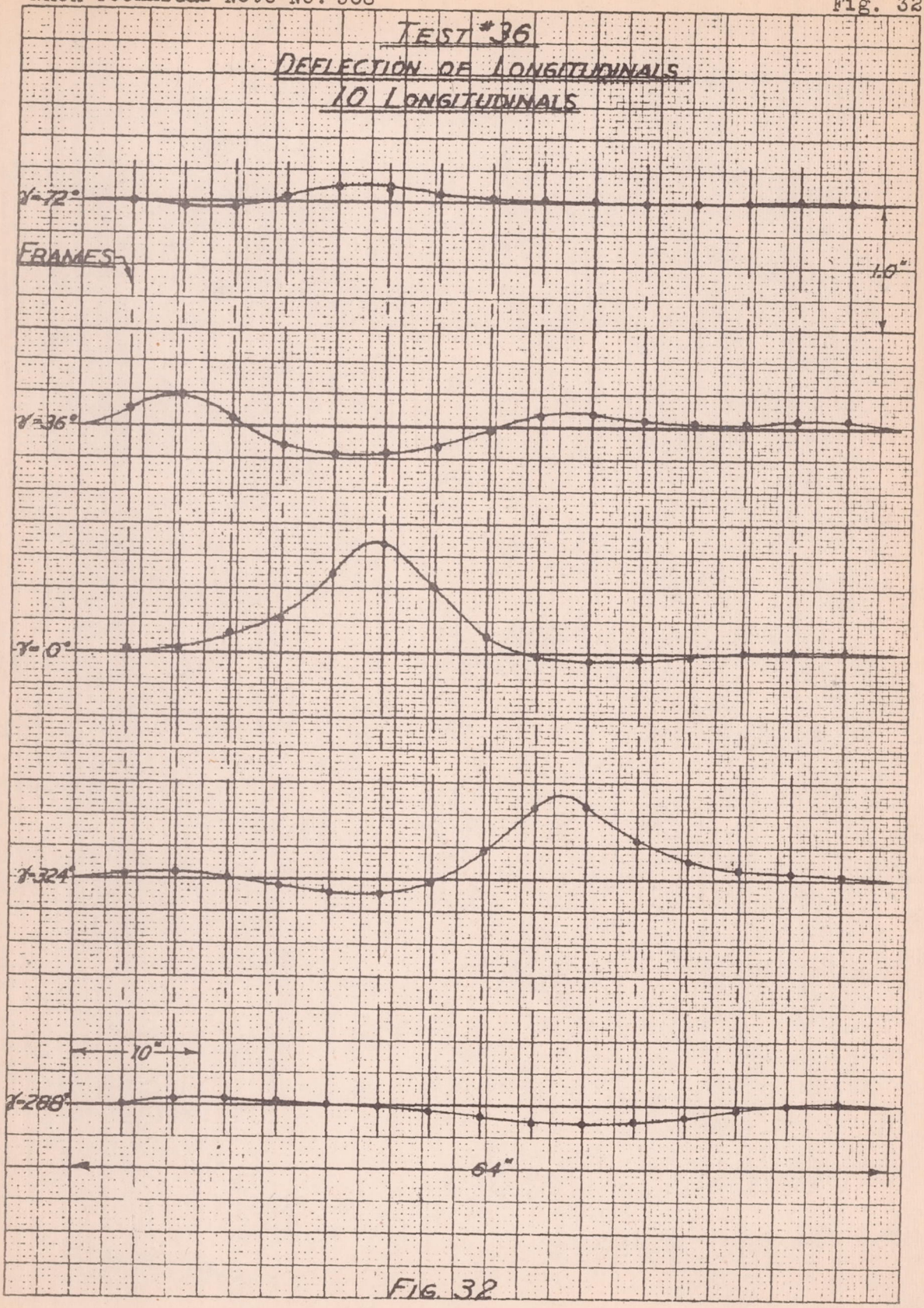
TEST #36
DEFLECTION OF LONGITUDINALS
10 LONGITUDINALS
γ=72°
FRAMES
1.0"
γ=36°
γ=0°
γ=324°
10"
γ=288°
64"

FIG. 32

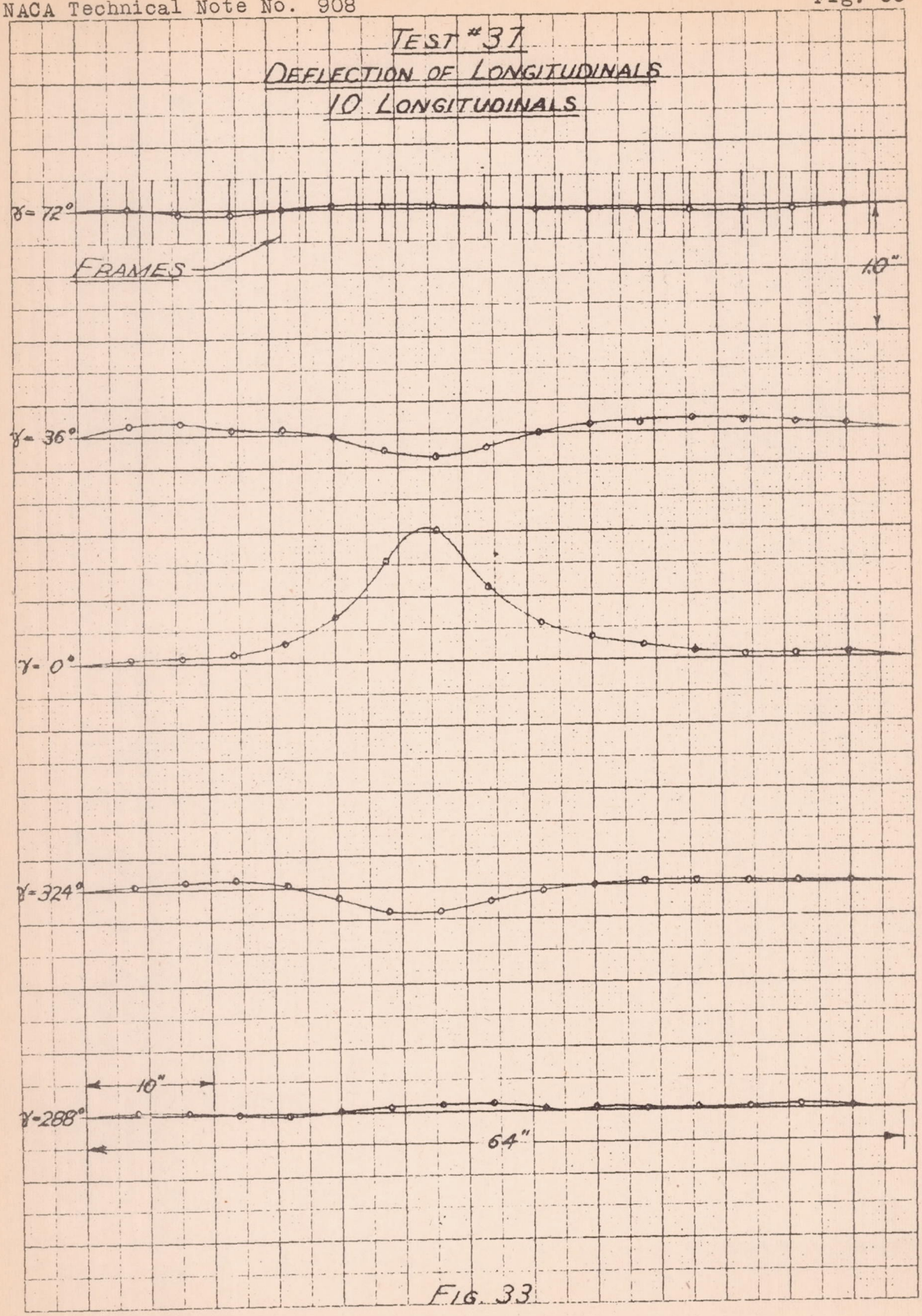
TEST #37
DEFLECTION OF LONGITUDINALS
10 LONGITUDINALS
γ= 72°
FRAMES
1.0"
γ= 36°
γ= 0°
γ=324°
10"
γ=288°
64"

FIG. 33

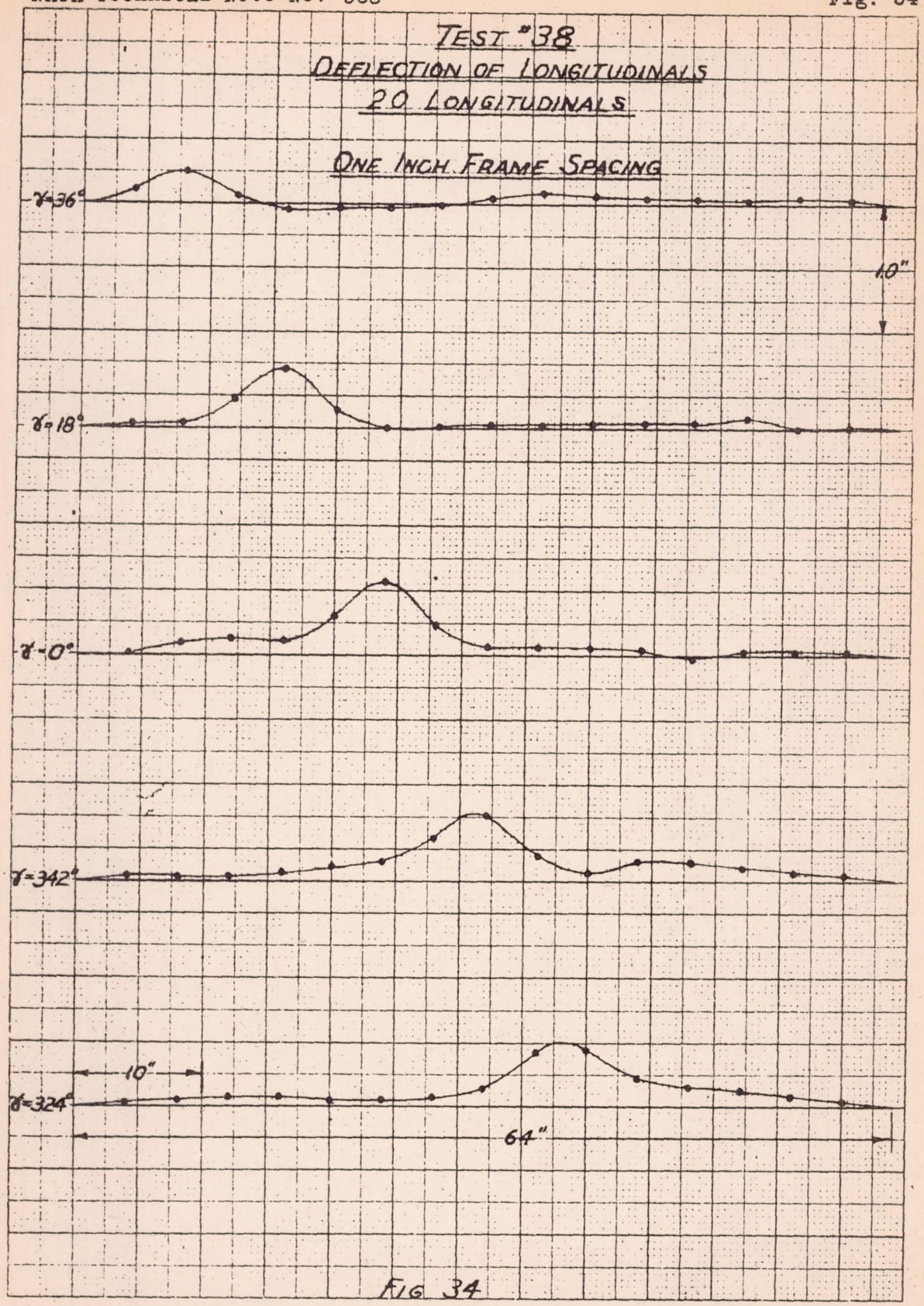
TEST "38
DEFLECTION OF LONGITUDINALS
20 LONGITUDINALS
ONE INCH FRAME SPACING
γ=36°
1.0"
γ=18°
γ=0°
γ=342°
γ=324°
10"
64"

FIG 34

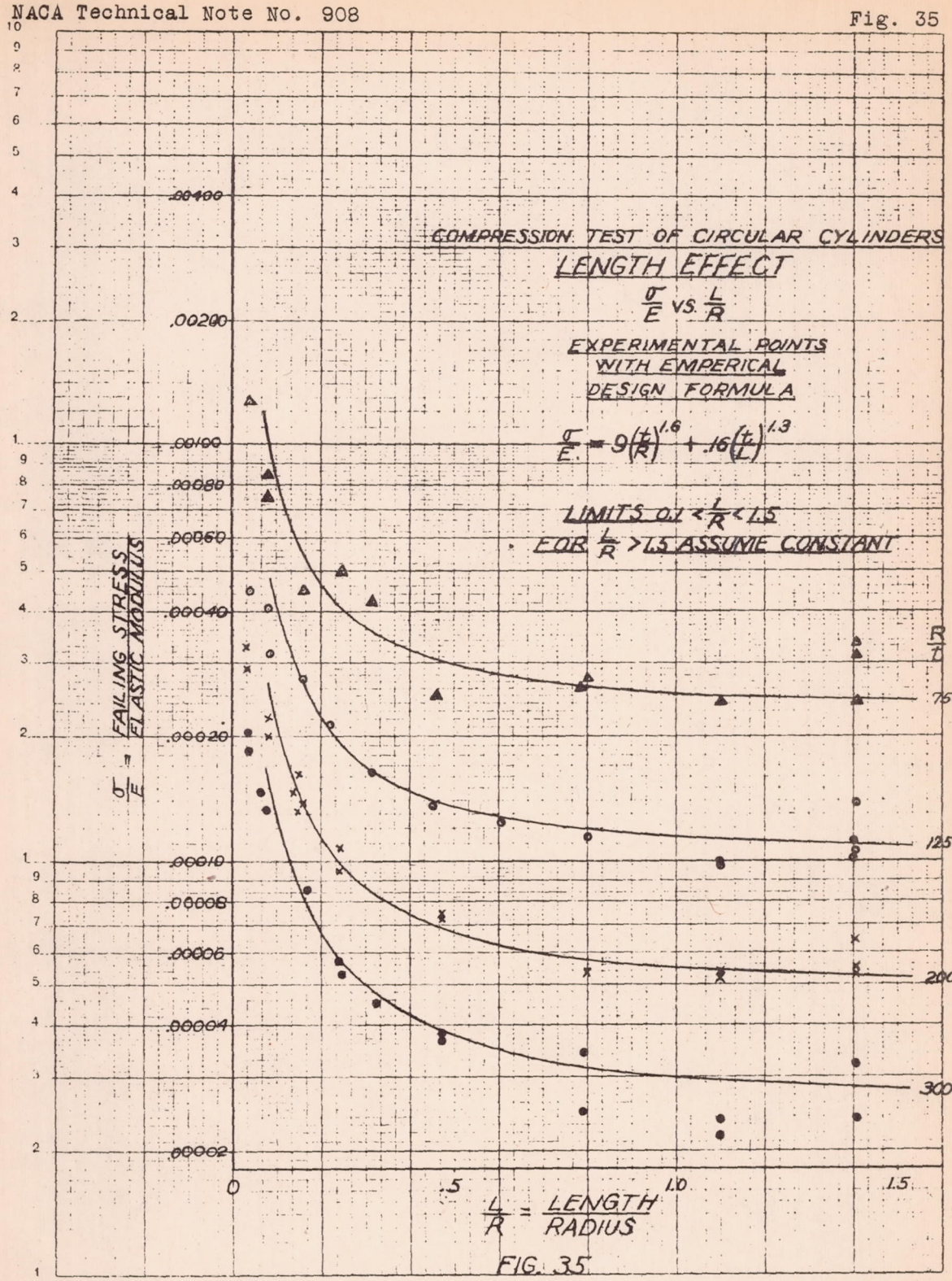
COMPRESSION TEST OF CIRCULAR CYLINDERS
LENGTH EFFECT
σ/E VS. L/R
EXPERIMENTAL POINTS WITH EMPERICAL DESIGN FORMULA
σ/E = 9(t/R)^1.6 + .16(t/L)^1.3
LIMITS 0.1 < L/R < 1.5
FOR L/R > 1.5 ASSUME CONSTANT
σ/E = FAILING STRESS / ELASTIC MODULUS
R/t
750
1250
2000
3000
.00400
.00200
.00100
.00080
.00060
.00040
.00020
.00010
.00008
.00006
.00004
.00002
0
.5
1.0
1.5
L/R = LENGTH / RADIUS

FIG. 35

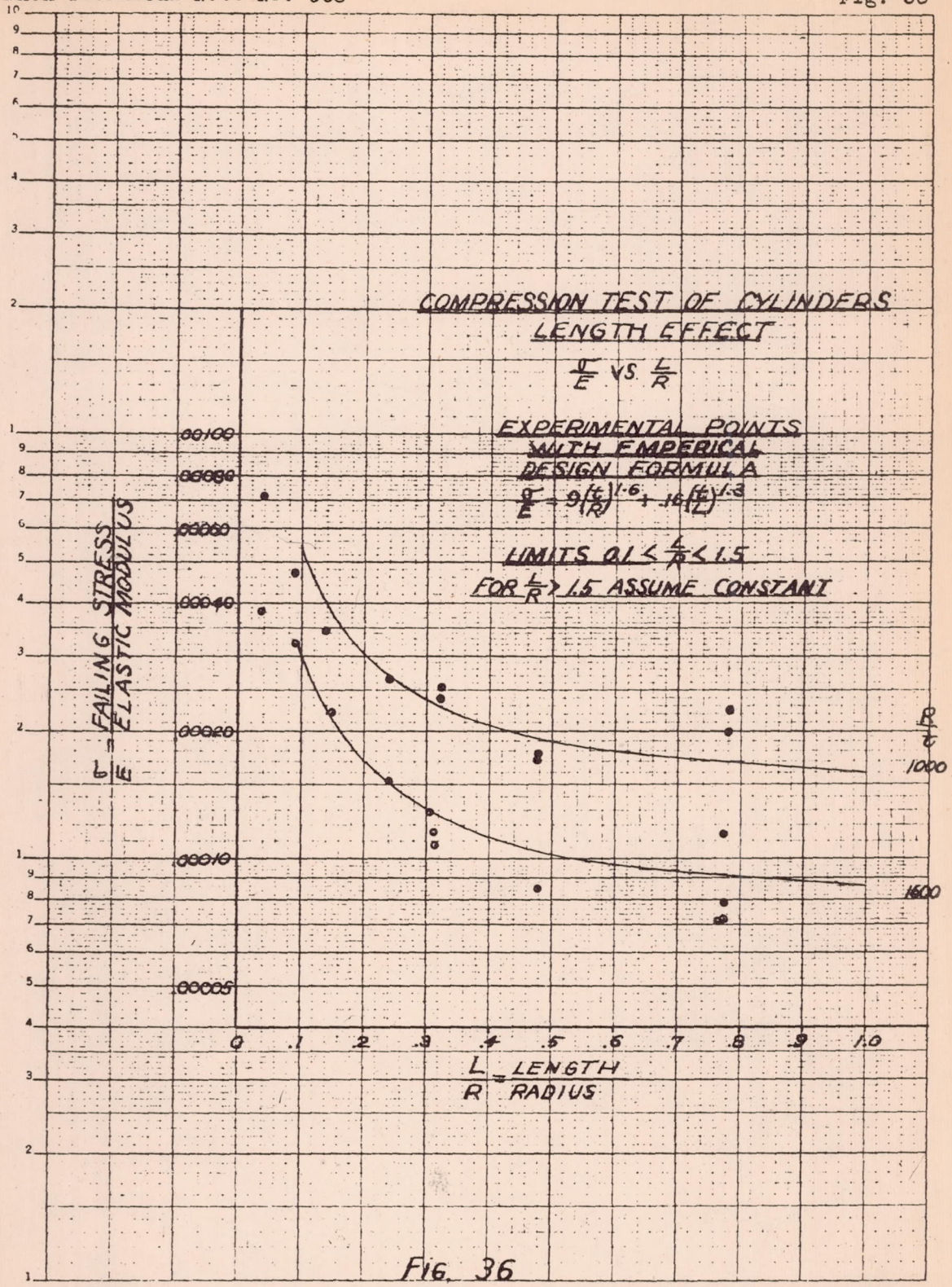
COMPRESSION TEST OF CYLINDERS
LENGTH EFFECT
$\frac{\sigma}{E}$ VS $\frac{L}{R}$
EXPERIMENTAL POINTS WITH EMPERICAL DESIGN FORMULA
$\frac{\sigma}{E} = 9\left(\frac{t}{R}\right)^{1.6} + 16\left(\frac{t}{L}\right)^{1.3}$
LIMITS $0.1 \leq \frac{L}{R} \leq 1.5$
FOR $\frac{L}{R} > 1.5$ ASSUME CONSTANT
$\frac{\sigma}{E}$ = FAILING STRESS / ELASTIC MODULUS
.00100
.00080
.00060
.00040
.00020
.00010
.00005
$\frac{R}{t}$
1000
1600
0 .1 .2 .3 .4 .5 .6 .7 .8 .9 1.0
$\frac{L}{R}$ = LENGTH / RADIUS

Fig. 36

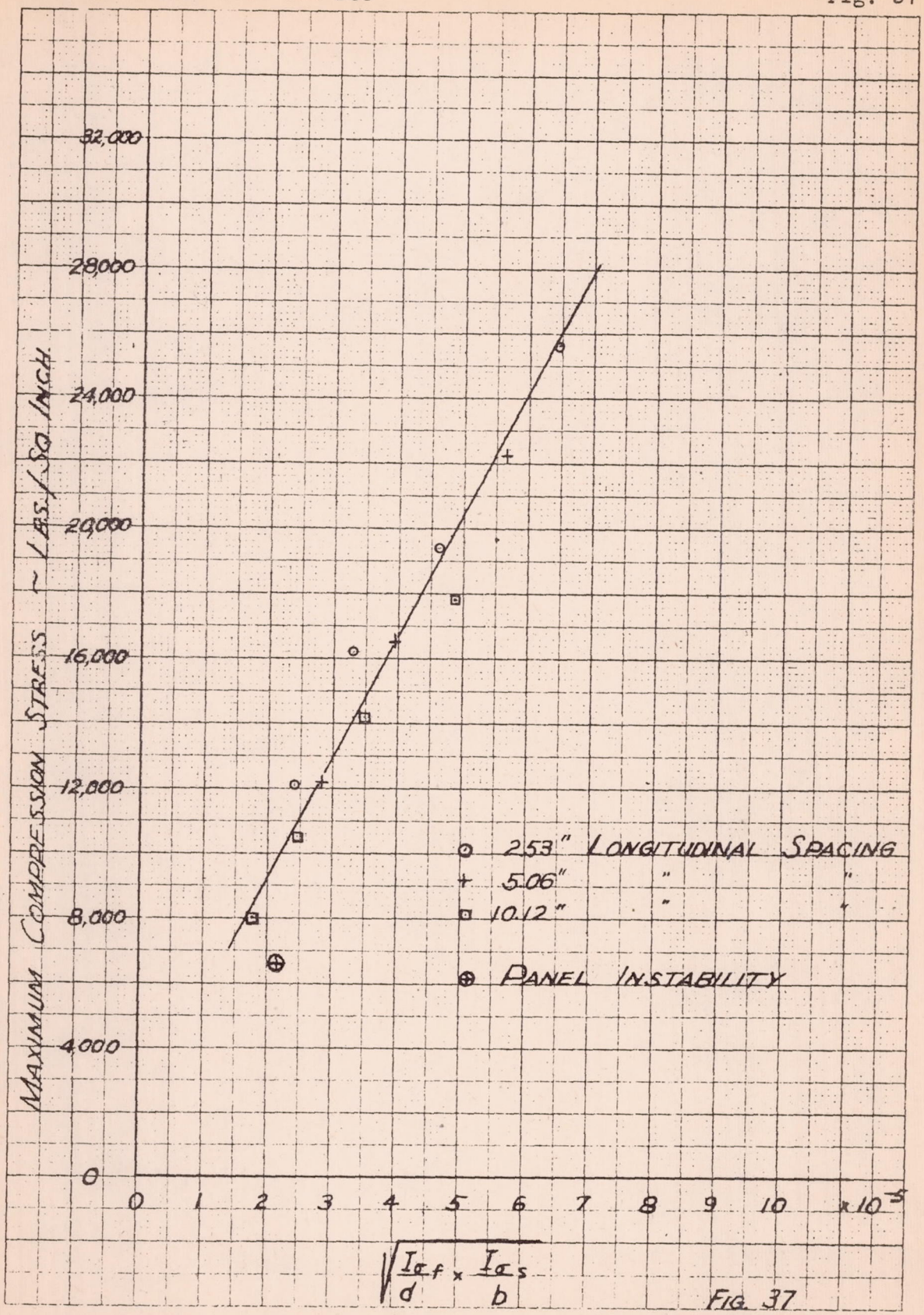
32,000
28,000
24,000
20,000
16,000
12,000
8,000
4,000
0
MAXIMUM COMPRESSION STRESS ~ LBS./SQ. INCH
0 1 2 3 4 5 6 7 8 9 10 ×10⁻⁵
√(Iσf/d × Iσs/b)
2.53" LONGITUDINAL SPACING
5.06" " "
10.12" " "
PANEL INSTABILITY

FIG. 37

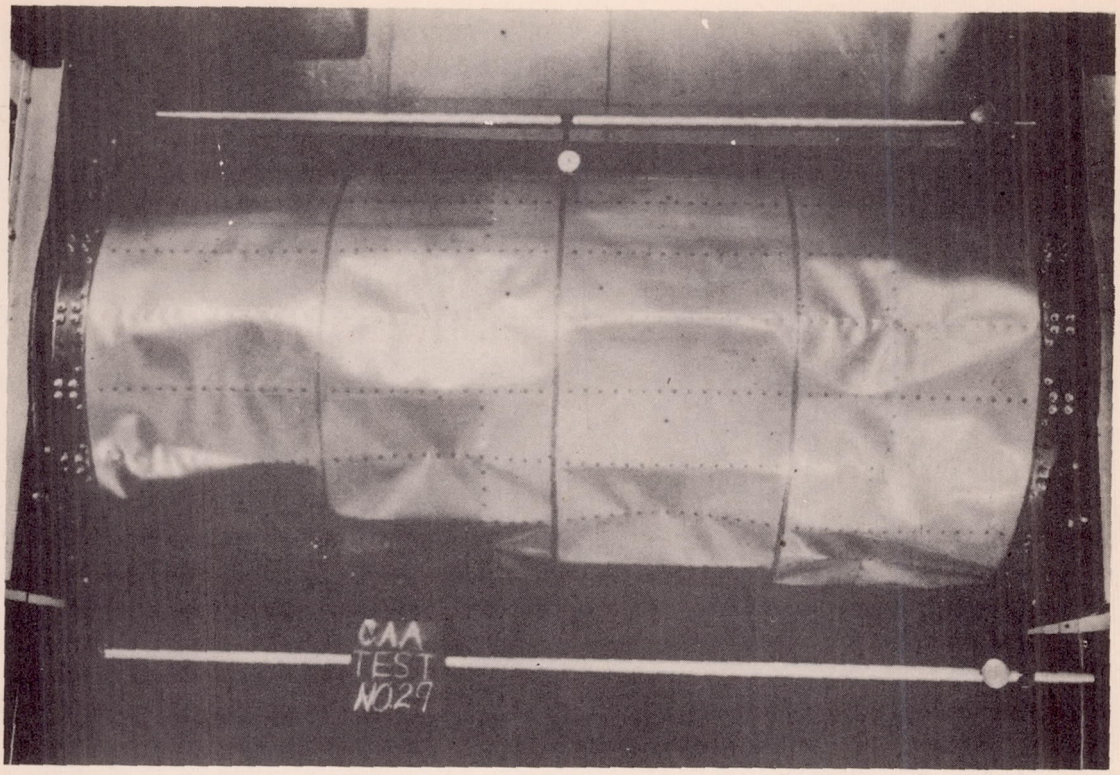

Fig. 38

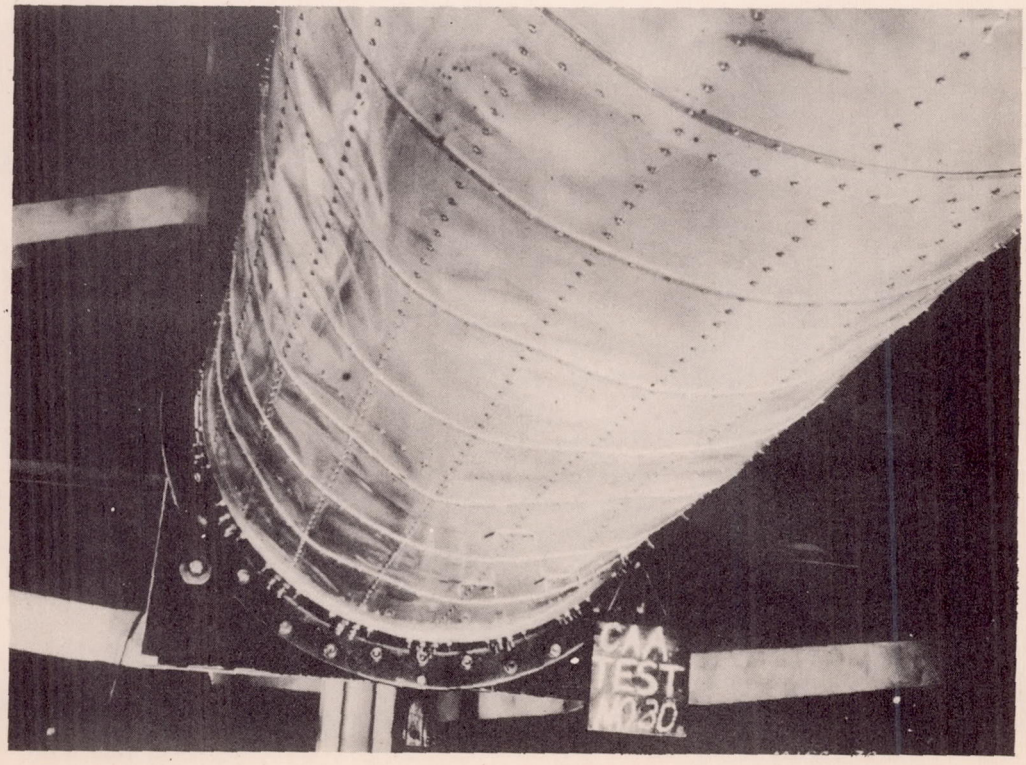

Fig. 39

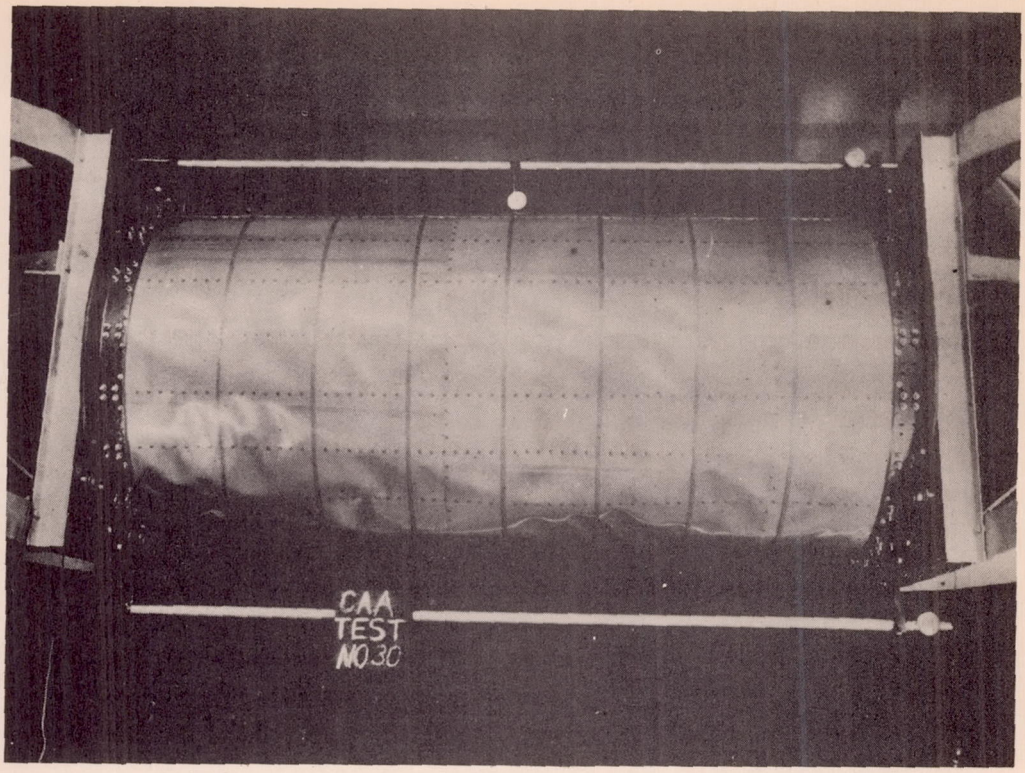

Fig. 40

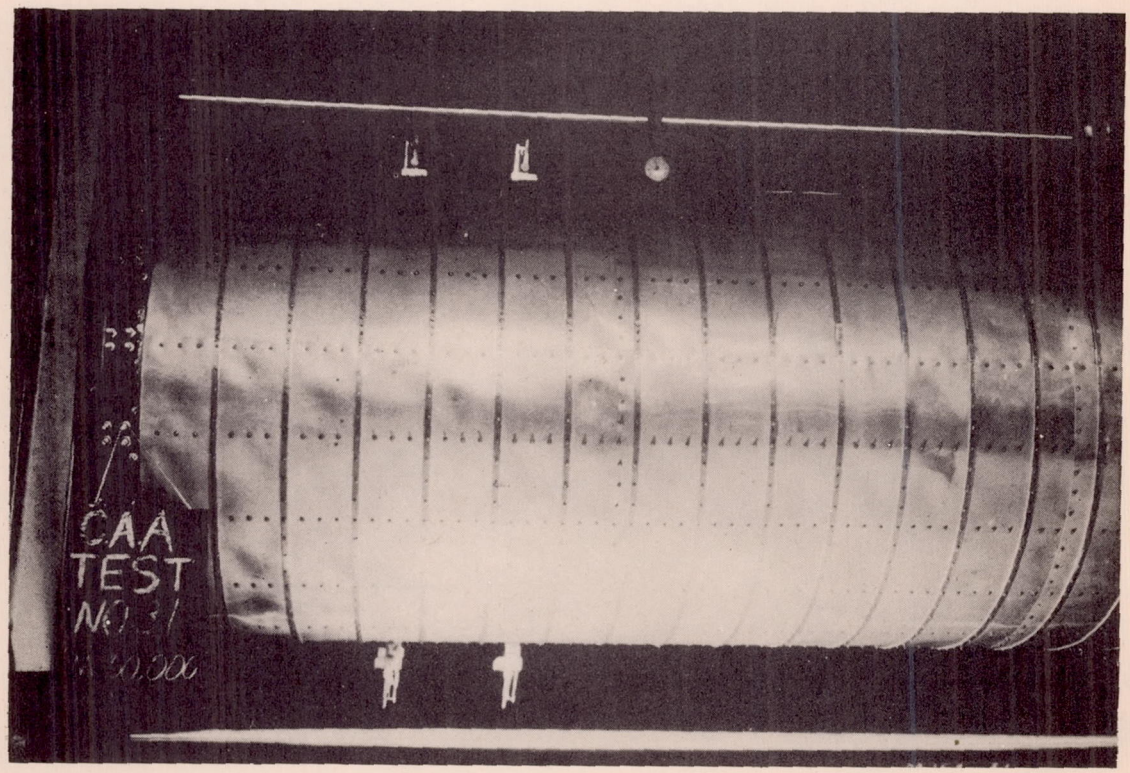

Fig. 41

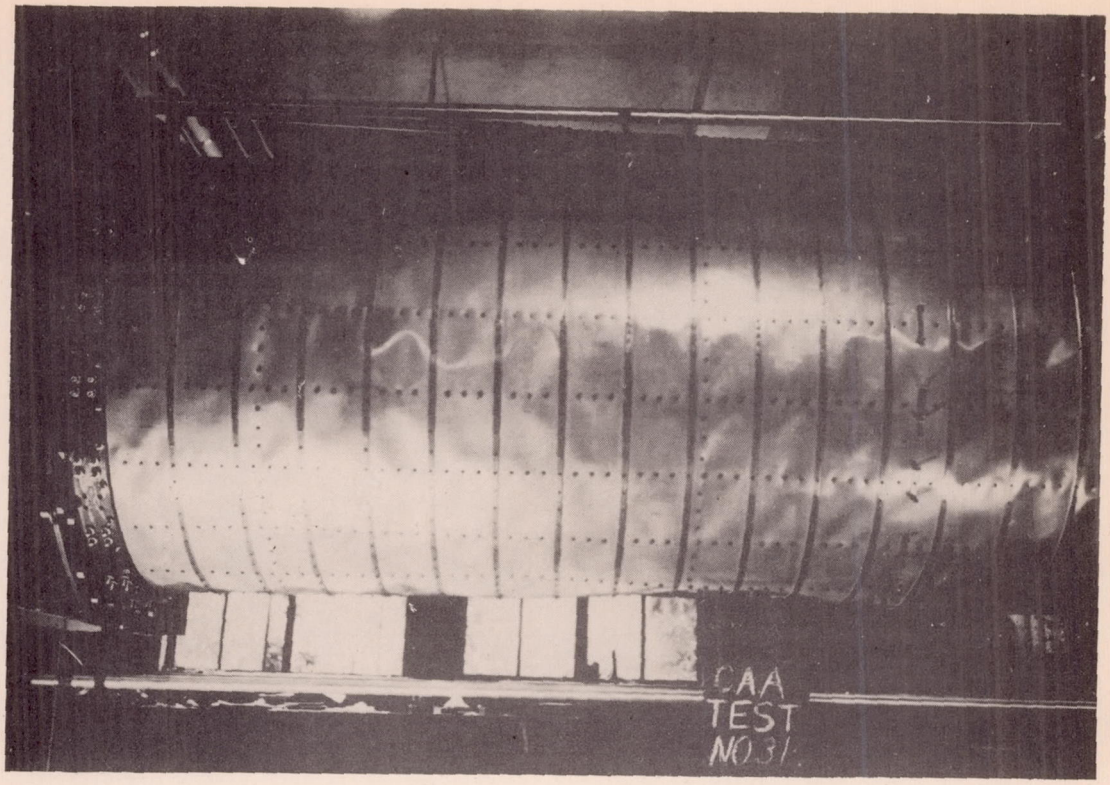

Fig. 42

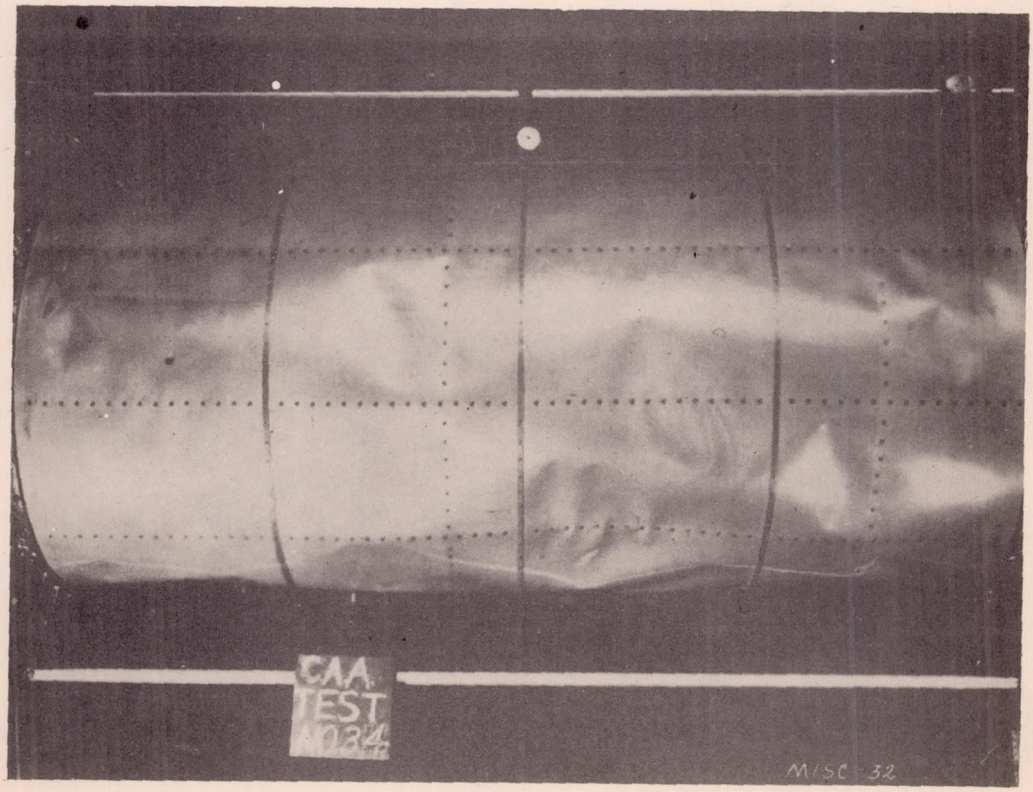

Fig. 43

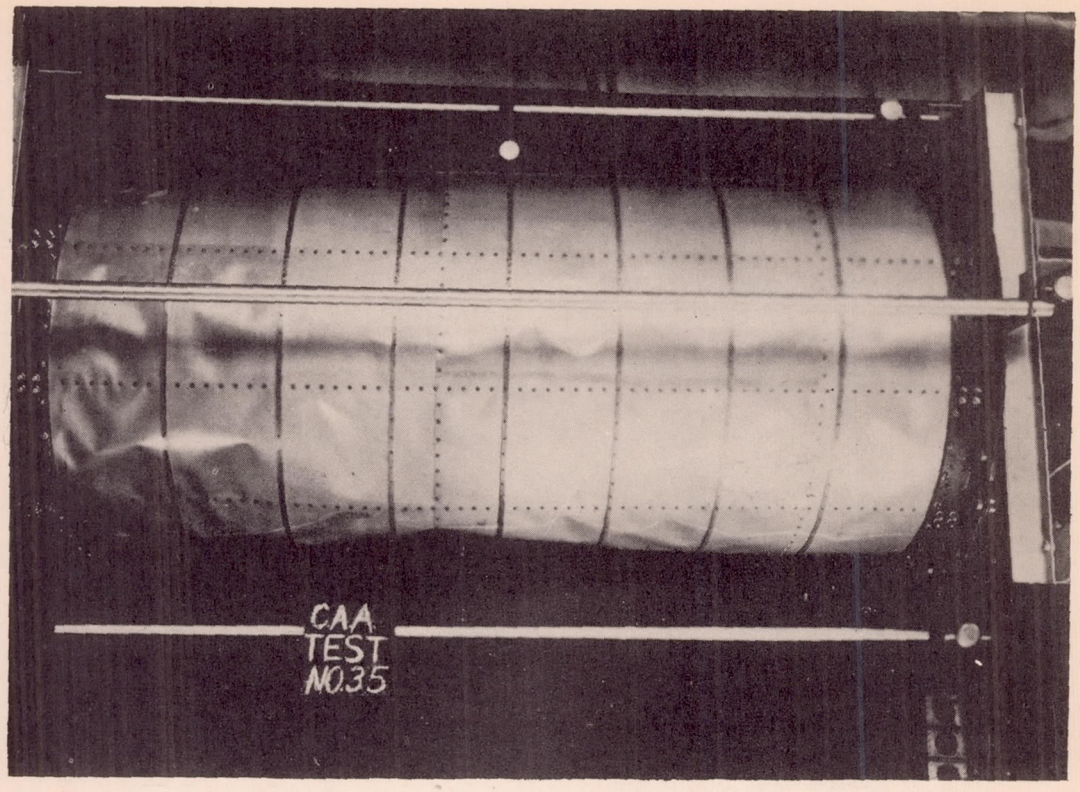

Fig. 44

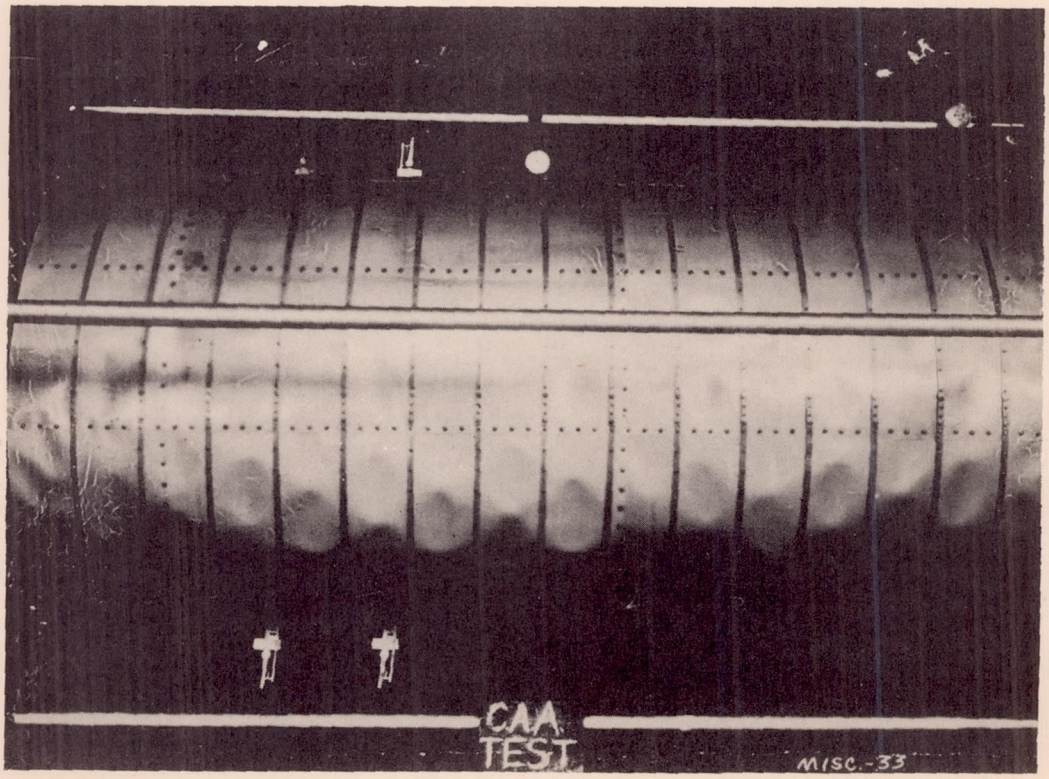

Fig.45

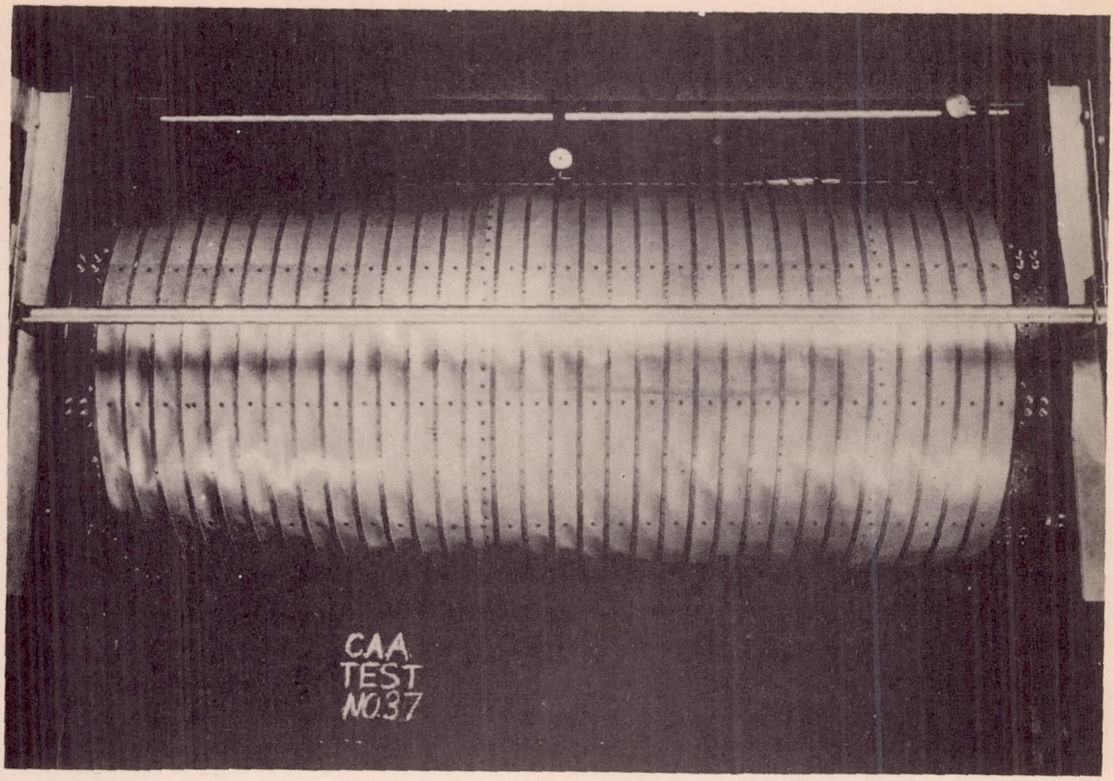

Fig. 46

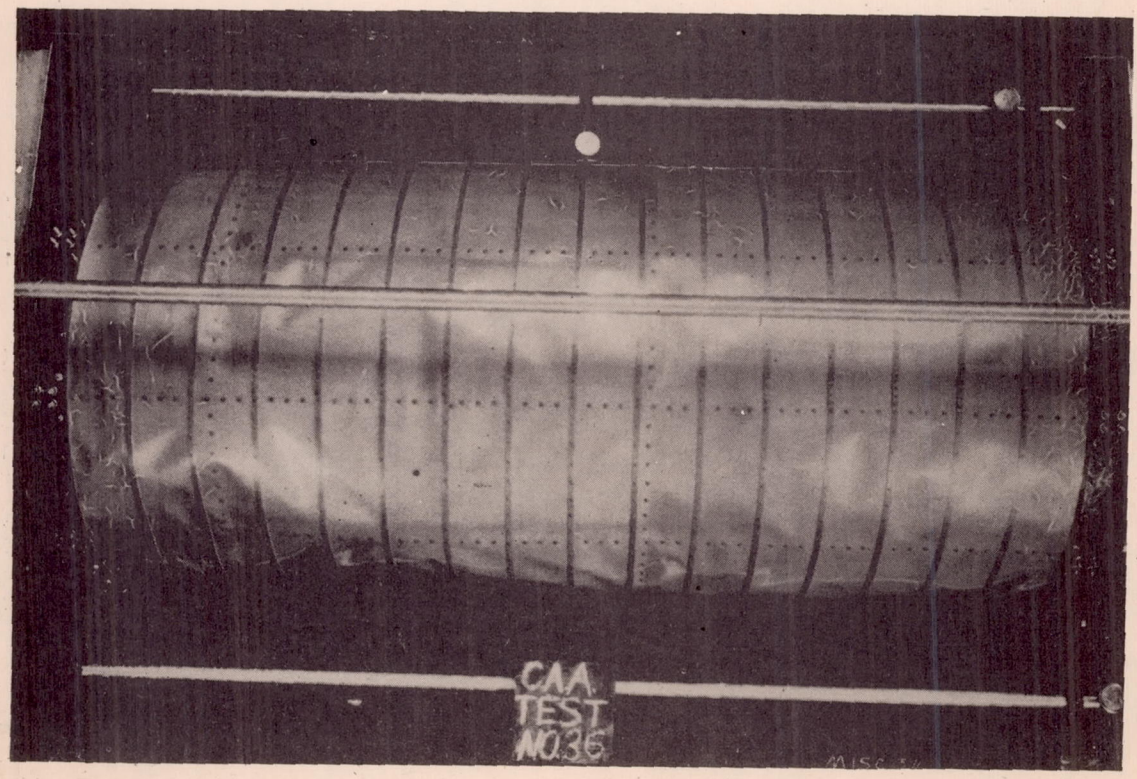

Fig. 47

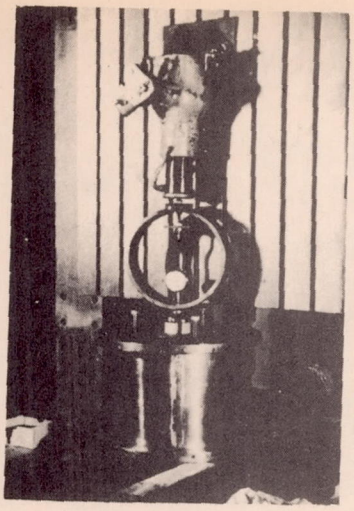

Fig. 48
Test Apparatus with
Specimen in Position.

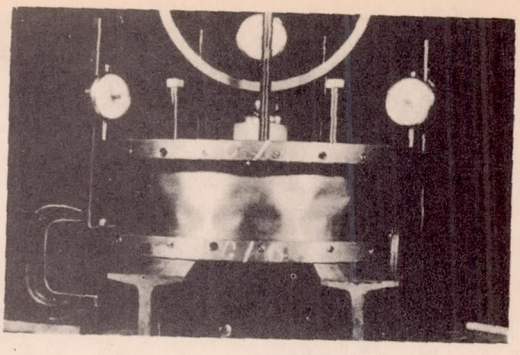

Fig. 49
Assembled Cylinder

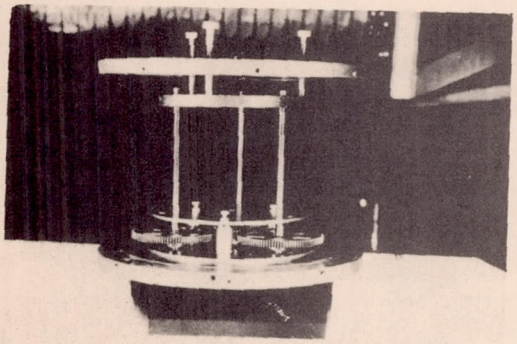

Fig. 50
Head Lowering
Mechanism.

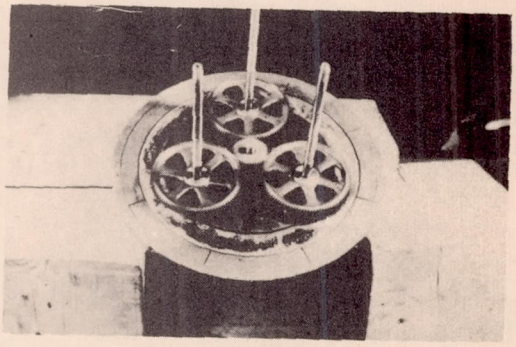

Fig. 51
Gear System

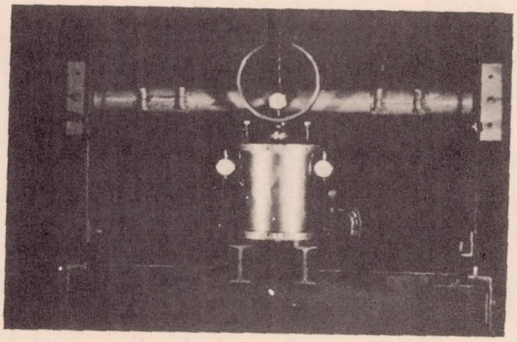

Fig. 52
Loading Apparatus

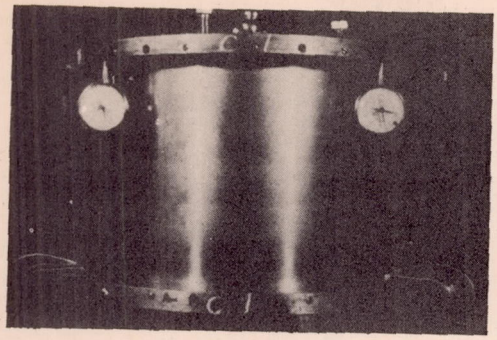

Fig. 53

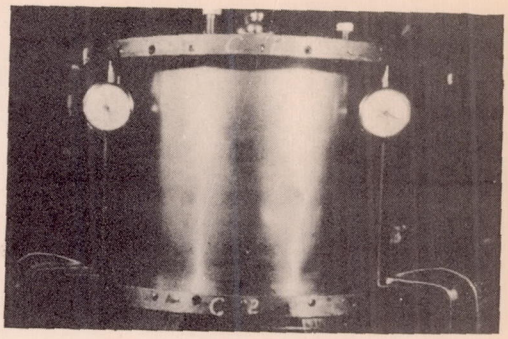

Fig. 54

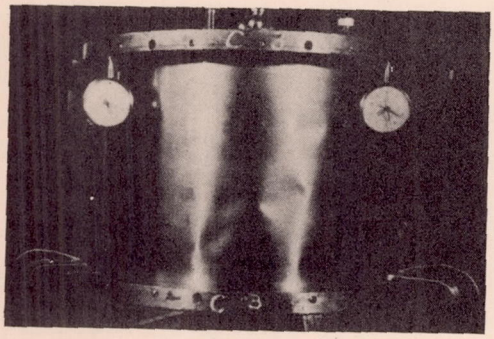

Fig. 55

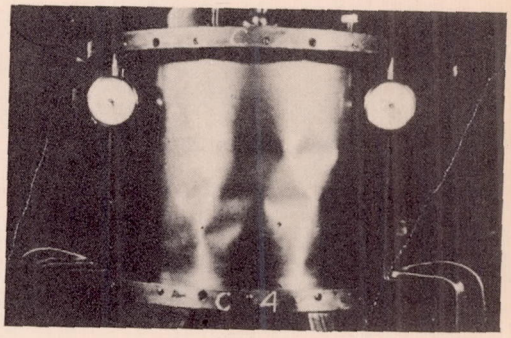

Fig. 56

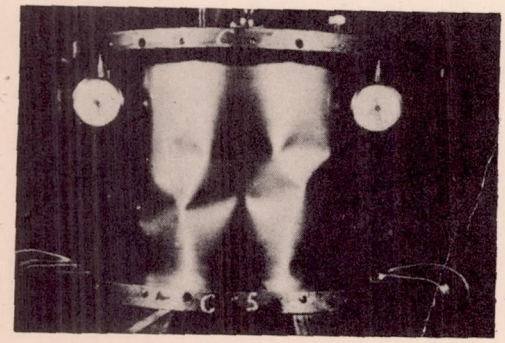

Fig. 57

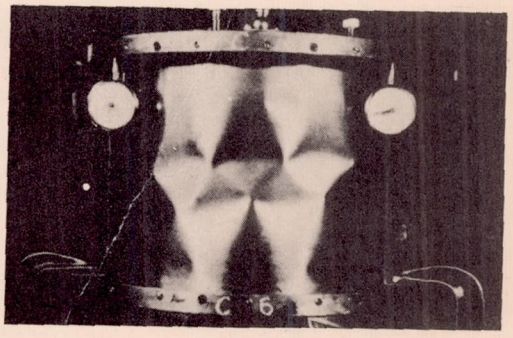

Fig. 58

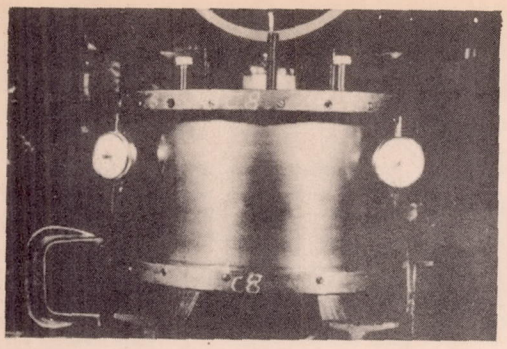

Fig. 59

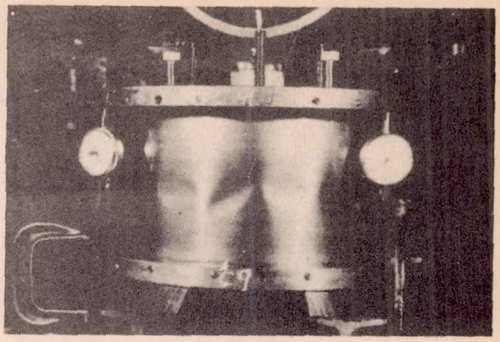

Fig. 60

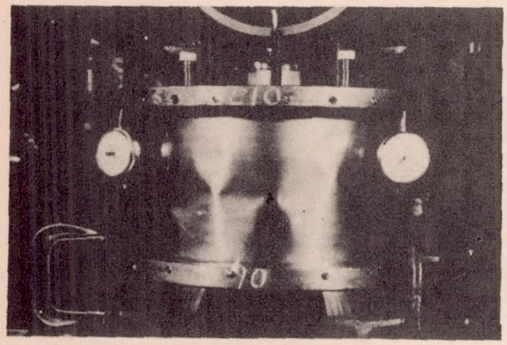

Fig. 61

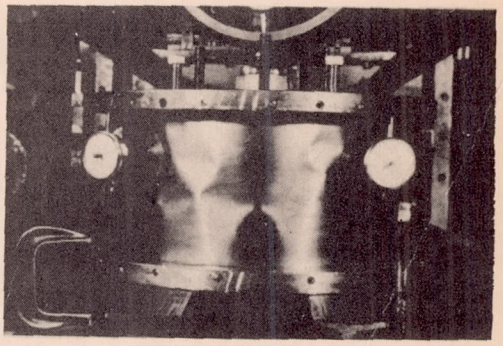

Fig. 62

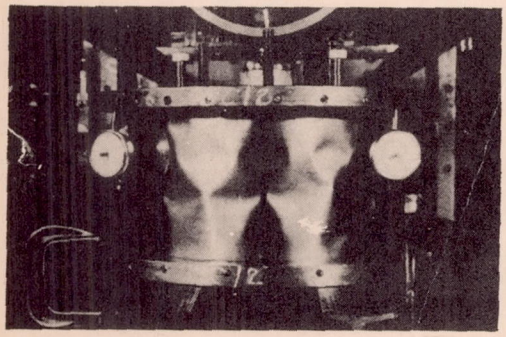

Fig. 63

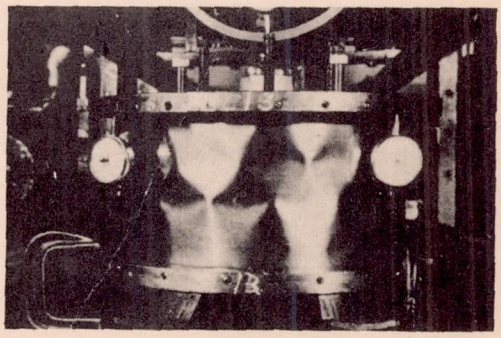

Fig. 64